OTH 92 363

HSE
Health & Safety Executive

SUMMARY REPORT ON AN INVESTIGATION INTO THE CORRELATION BETWEEN FULL-SCALE MEASURED AND PREDICTED MOTIONS OF THE SSSV 'UNCLE JOHN'

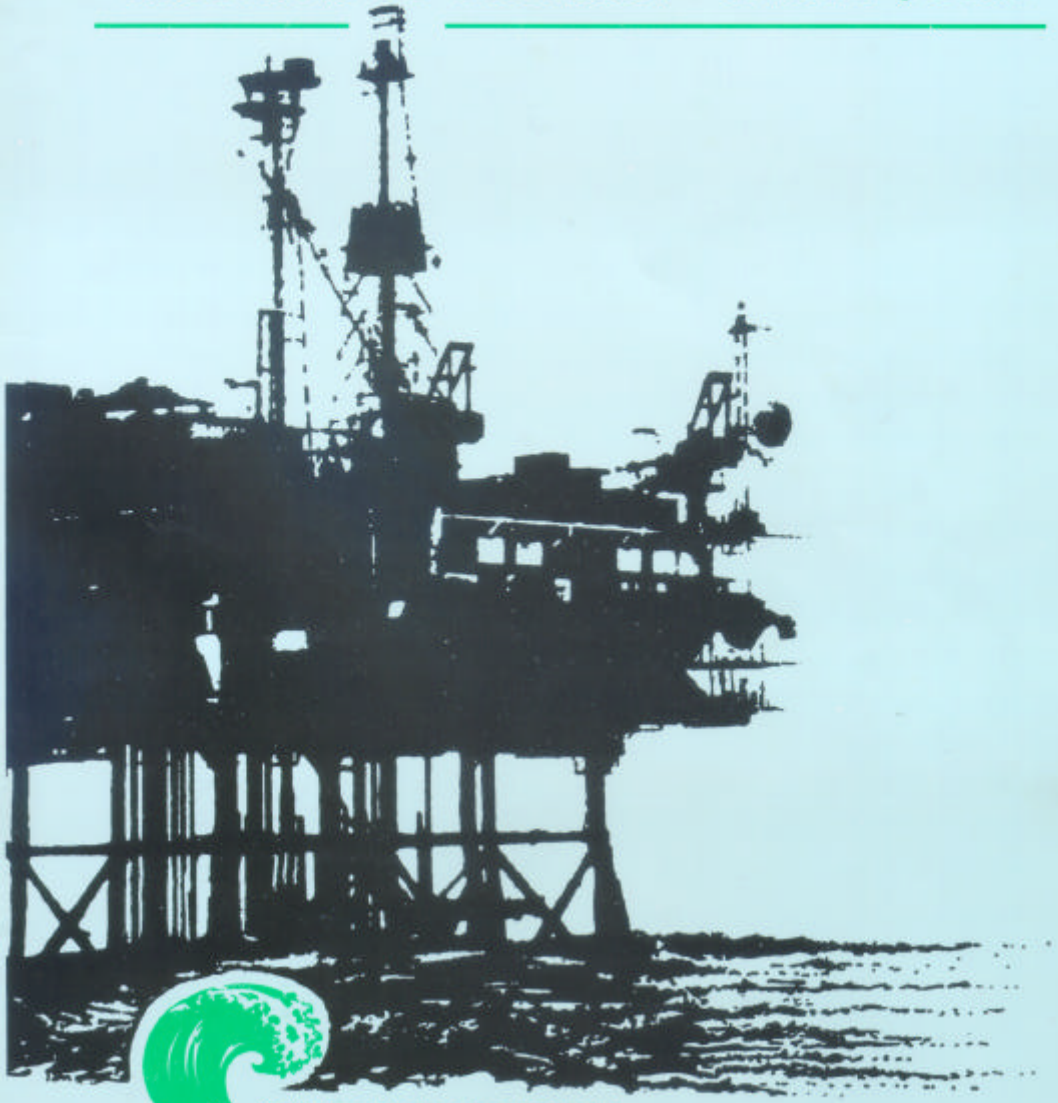

Offshore Technology Report

Health and Safety Executive

OTH 92 363

SUMMARY REPORT ON AN INVESTIGATION INTO THE CORRELATION BETWEEN FULL-SCALE MEASURED AND PREDICTED MOTIONS OF THE SSSV 'UNCLE JOHN'

Authors

R G Standing, W J Brendling and G E Jackson

BMT Fluid Mechanics Limited
Orlando House
1 Waldegrave Road
Teddington
Middlesex TW11 8LZ

London: HMSO

Health and Safety Executive - Offshore Technology Report

First published 1993
ISBN 0 11 882136 9

This report is published by the Health and Safety Executive as part of reports of work which has been supported by funds formerly provided by the Department of Energy and lately by the Executive. Neither the Executive, the Department nor the contractors concerned assume any liability for the reports nor do they necessarily reflect the views or policy of the Executive or the Department.

Results, including detailed evaluation and, where relevant, recommendations stemming from their research projects are published in the OTH series of reports.

Background information and data arising from these research projects are published in the OTI series of reports.

FOREWORD

BMT Fluid Mechanics has carried out a series of investigations for the Department of Energy into the motions of the Semi-Submersible Support Vessel 'Uncle John'. These investigations started with a programme of measurements on board the vessel while it was operating in the Danish sector of the North Sea during March and April 1987. These measurements were then analysed, and first-order response amplitude operators and statistics were compared with predictions using NMIWAVE diffraction computer program and with existing model test data. A subsequent investigation made similar comparisons of low-frequency motions, combining both second-order wave loading and wind gust loading into numerical simulations using the BMTSPM computer program.

The present Summary Report has been prepared in camera-ready format for publication by Her Majesty's Stationery Office, according to specifications attached as Appendix B to the AEA Technology Agreement, dated August 1990, issue 2. The BMT Fluid Mechanics Ltd proposal for this work was presented to the Department of Energy on 6 February 1991. The contract for preparing this Summary Report is contained in AEA Technology Agreement no E/5B/CON/8313/2722, dated 13 September 1991.

CONTENTS

SUMMARY

Motions of the SSSV 'Uncle John' were measured while the vessel was operating in the North Sea. Wave-frequency and low-frequency components of these motions were compared separately with numerical predictions and with laboratory data.

Wave-frequency motions were found to correlate well with predictions from the NMIWAVE wave diffraction program. Difference between response amplitude operators obtained from the full-scale and laboratory data at high frequencies were attributed to effects of wave directional spreading.

Low-frequency motions were compared with a theoretical model which combined low-frequency wind gust loads and second-order wave forces, calculated under inviscid potential-flow assumptions. The model represented response characteristics of the full-scale vessel, including its heave, roll and pitch damping, and the dynamic positioning control system with thruster force limits.

The theoretical model predicted low-frequency heave motions very well in higher sea states, and up to 50 percent of the measured surge and sway responses. These calculated motions were due mainly to second-order wave loads. Wind gust loads in the surge and sway directions were significant, but were largely balanced by the vessel's ‘wind feed forward' system. Wind loads accounted for at most 30 to 50 percent of the vessel's roll and pitch responses.

The numerical model often underestimated the vessel's response motions, and this was probably due to a combination of: viscous drag forces, which were not represented at all in the theoretical model; inaccuracy in modelling features of the thruster and control systems, in particular delays introduced by thruster action and filtering; differences between wind forces acting of the actual vessel and those calculated by its 'wind feed forward' system; low-frequency swell waves, which could not be measured reliably; uncertainties in the amount of damping present and numerical modelling uncertainties.

1. INTRODUCTION

Mathematical and physical models are often used during the design of offshore structures to estimate wave loads and wave-induced motions. It is comparatively rare, however, to undertake detailed full-scale measurements of vessel motions after the vessel has been commissioned, and to correlate these measurements with numerical predictions and with model test results. The adequacy of the design procedures and assumptions is therefore largely unknown, and improvements which could in principle come from operational measurements are not made.

Two earlier investigations into full-scale and predicted motions of semi-submersible platforms were reported by Olsen and Verlo (1976) and by Mørch, Kaasen and Rudi (1983). The first of these papers was concerned with first-order, wave-frequency motions and structural stresses; the second with transient motions and damping. Both papers reported reasonable agreements between the measured and simulated results.

In early 1987 BMT Fluid Mechanics Ltd carried out a programme of measurements on board the Semi-Submersible Support Vessel 'Uncle John', then owned by Houlder Offshore Ltd, while it was operating in the North Sea. The motions of the vessel in surge, sway, heave, roll and pitch were measured, together with environmental data (wave height, wind speed and direction) and various signals from the vessel's dynamic positioning controller.

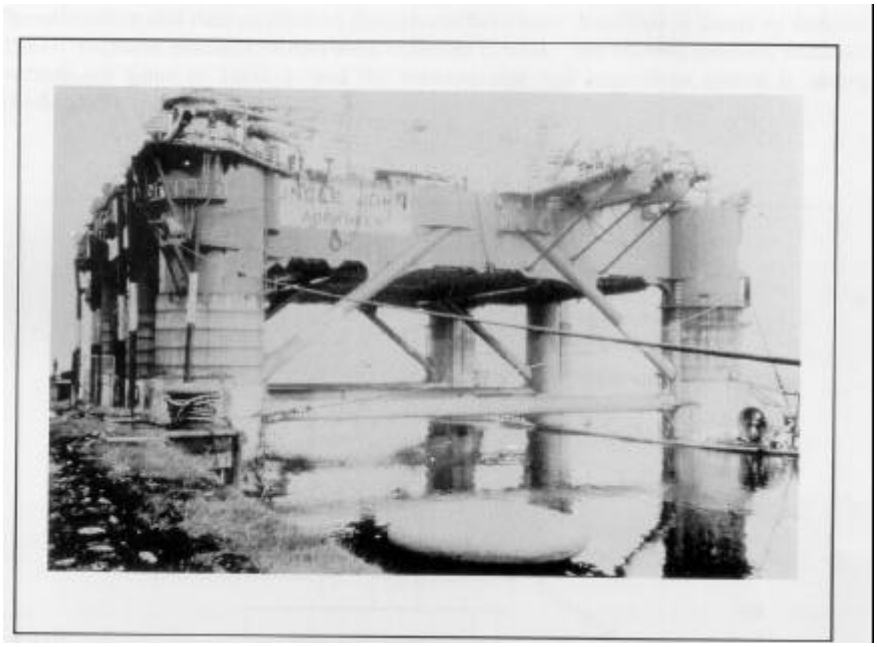

Figure 1
The SSV 'Uncle John'

Houlder (1981) has described the main features of the vessel, shown in Figure 1. In an earlier investigation Haavie and English (1978) indicated reasonable agreement between full-scale and model measurements of significant response motions. BMT had performed extensive model tests during the vessel's design, and had carried out subsequent numerical investigations. The model tests included measurements of wind force and moments coefficients in a wind tunnel, and measurements of vessel motions and wave drift forces in a wave basin.

1.1 OBJECTIVES

The initial aims of this project were stated to be as follows (Every, 1988). The project was 'to give designers an indication of where present design techniques do not fully predict the wave frequency motions of full-scale operational vessels. From the safety point of view the motions of the vessel were to be quantified and deviations from expected excursions identified. For the operator the experiment was to yield information on exactly how the vessel was performing compared to his expectations.'

A further phase (Brendling and Standing, 1990) was 'intended to extend the previous work by investigating the low-frequency response of the 'Uncle John', and to compare the measured low-frequency motions with those predicted by numerical techniques.'

2. MEASUREMENT PROGRAMME

The full-scale measurement programme and data acquisition system have been described by Jackson (1987), and in an abridged published form by Jackson and Wilson (1988).

The 'Uncle John' was equipped with a Colnbrook Instruments Motion Monitoring Package, the output from which included vessel accelerations together with motions in surge, sway, heave, roll and pitch. A preliminary analysis was carried out on board the vessel, and the information was recorded on magnetic tape for detailed analysis ashore.

Wave elevation was measured using a Datewell Waverider buoy, moored some 500m from the vessel, while wave direction was established by visual observation. Wind speed and direction were also measured, using the anemometer system already installed on the vessel.

The 'Uncle John' is dynamically positioned, and much of the available information from the dynamic positioning (DP) control system was also recorded. This information was not used during the initial wave-frequency analysis, but proved essential during the subsequent low-frequency investigation.

A Braystoke propeller current meter was used on several occasions to measure the current speed and direction, but the current in the work area was found to be only 0.1 to 0.3 knots, which proved to be at the low end of the operating range of the meter.

The calibration and data acquisition procedures have been described in detail by Jackson (1987). Eighteen channels of data were collected in total. The channel numbers and their contents are listed in Table 1, and the measurement and acquisition system is shown schematically in Figure 2.

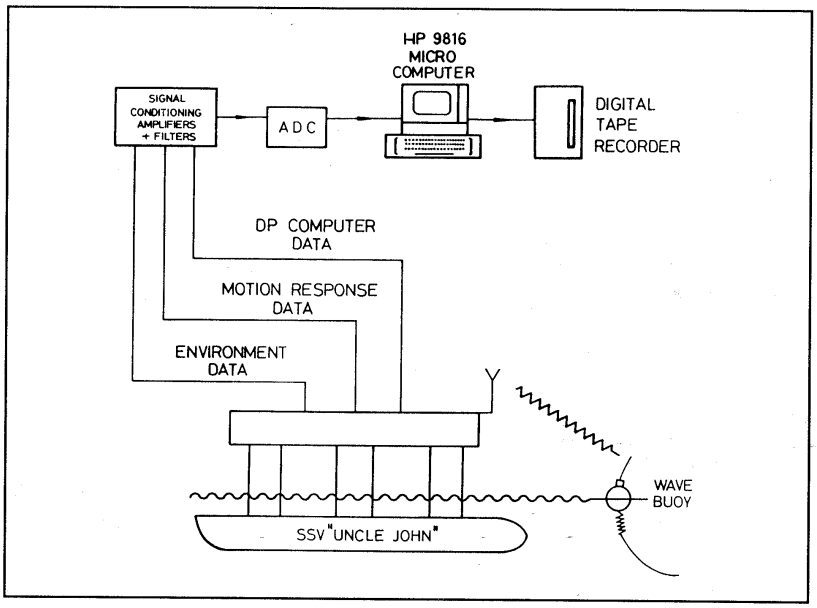

Figure 2
Schematic diagram of on-board instrumentation

Table 1
List of data channels

Channel no.	Measurement	Units
1	Wave height	m
2	Wind speed	m/s
3	Wind direction	degrees
4	Roll angle	degrees
5	Pitch angle	degrees
6	Yaw acceleration	degrees s^{-2}
7	Surge	m
8	Sway	m
9	Heave	m
10	Roll acceleration	degrees s^{-2}
11	Pitch acceleration	degrees s^{-2}
12	DP surge error	m
13	DP sway error	m
14	DP yaw error	degrees
15	DP surge force	tonne f
16	DP sway force	tonne f
17	Target heading	degrees
18	Heading integrator	tonne f m

The 'Uncle John' was relatively inaccessible from shore support, and so data and equipment reliability were of major concern. A full duplicate set of all instrumentation was therefore carried, and a BMT engineer was on board the vessel during the entire measurement programme. As a result this programme of measurements has produced a very reliable set of data, recorded over a period of 17 days.

The measurements took place during March and early April 1987, while the 'Uncle John' was engaged in operations in the Danish sector of the North Sea. Fortunately, from the point of view of the project, two severe storms occurred during this period. During the first of these storms the vessel had to move away from the work area, and was at a survival draught of 13 m without dynamic positioning control. The highest value of H_8 recorded during this period was 6.36 m. The second storm was less severe than the first, and did not stop diving operations, the highest value of H_8 being 3.64 m, and the vessel maintaining is operational draught of 15.5m.

A total of 177 seventy-minute runs were recorded, providing over 200 hours of data in all, and the significant wave height H_8 was greater than 2.0 m for over 50 percent of the time. Figure 3 shows the way in which the mean wind speed varied during the course of the measurement programme, and Figure 4 shows the corresponding graph of significant wave height.

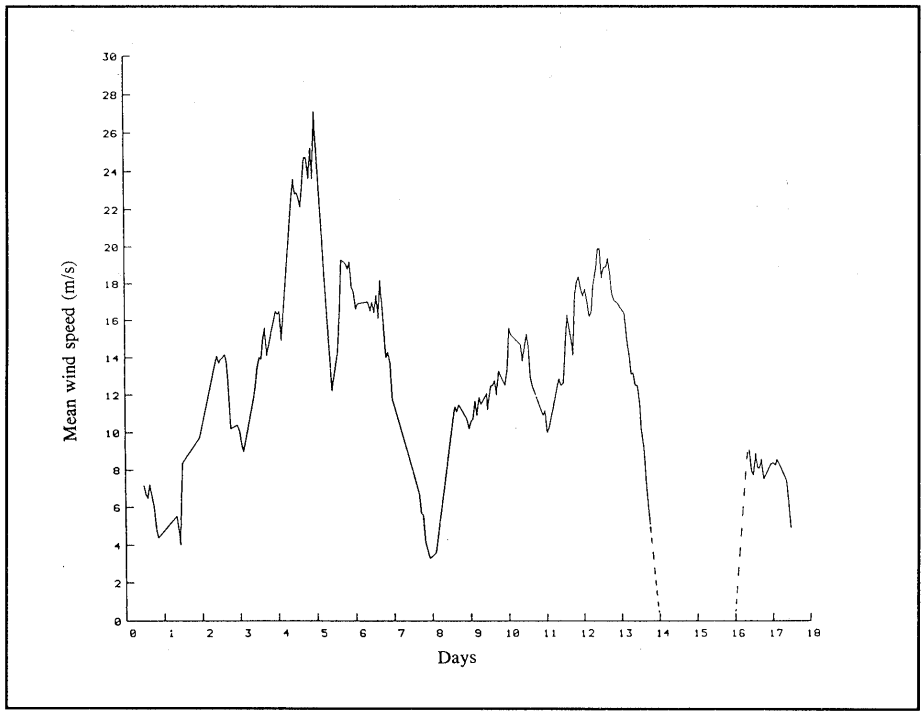

Figure 3
Mean wind speed during the measurement period

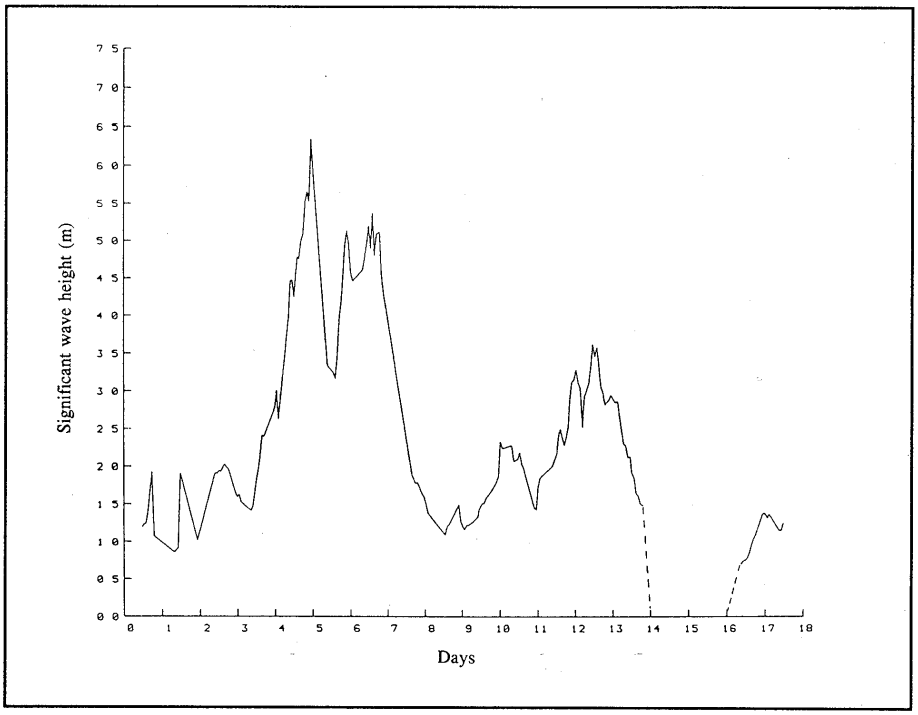

Figure 4
Significant wave height during the measurement period

Figure 5 shows the first 400 seconds of one typical set of recorded data, measured at the peak of the second storm when H_8 was 3.64 m. The 'stepped' character of the wind speed history is typical of records obtained via the vessel's DP system, which has a relatively low update rate on the output channels used. The vessel motion time-histories display a mixture of wave-frequency and low-frequency response, the latter being particularly noticeable on the surge and sway records. these particular measurements were obtained using the Colnbrook package. Alternative estimates of low-frequency surge and sway motions were obtained from the vessel's DP error detection system, and these alternative measurements were used in the subsequent low-frequency motion analysis.

2.1 VESSEL CONDITIONS

During the majority of the measurement programme the vessel was at its operational draught of 15.5 m. The vessel moved to a survival draught of 13.0 m, however, during the first of the two storms.

Principal particulars of the vessel in these two conditions were estimated to be as shown in Table 2.

The motion monitoring device was located at the plan centre of the vessel at a point 26.0 m above the keel. All motions shown in this report were calculated at this location.

The values in Table 2 come mainly from calculations, or from available data about the vessel. The centre of gravity, however, was estimated from the metacentric height, GM, recorded in the vessel's Soundings and Stability log at various times during the measurement programme.

Table 2
Principal particulars of the SSSV 'Uncle John'

	Operational	Survival
Overall length of pontoons	77.0 m	77.0 m
Width overall	52.6 m	52.6 m
Draught	15.5 m	13.0 m
Displacement	9,539 tonne	9,013 tonne
Height of centre of buoyancy above keel	4.96 m	4.42 m
Gyradii about centre of gravity:		
roll	22 m	22 m
pitch	19 m	19 m
yaw	25 m	25 m
Approximate natural periods:		
heave	20s	
roll	39s	
pitch	33s	
GM	2.15 to 2.53 m	2.46 m
Height of centre of gravity above keel	11.73 to 11.35 m	11.41 m

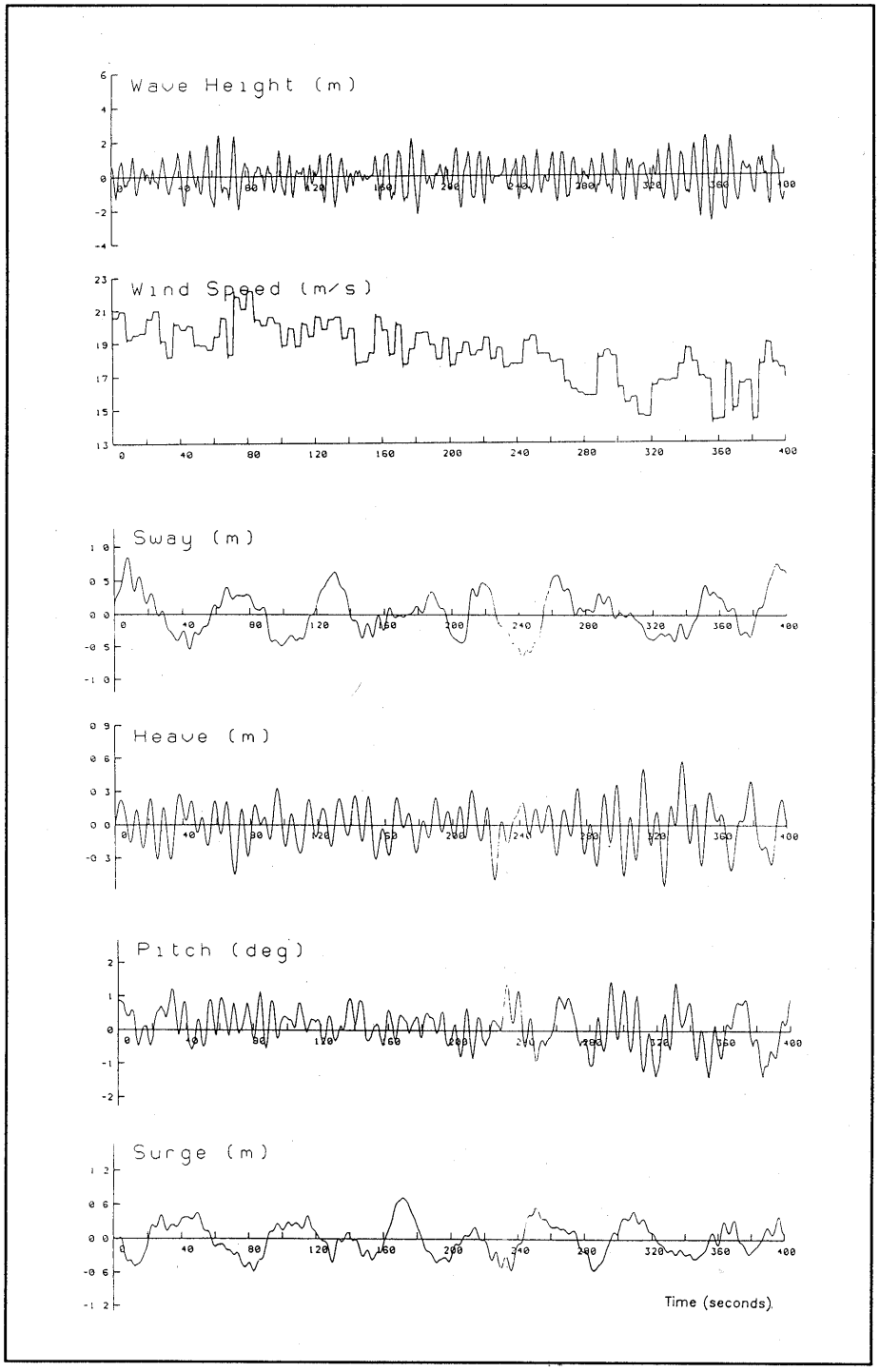

Figure 5
Sample time-histories (run 140): H8

3. WAVE-FREQUENCY MOTIONS

3.1 THE NUMERICAL MODEL

The numerical model used in the investigation of wave-frequency motions is known as NMIWAVE. This program is based on first-order wave diffraction theory and the source/sink approach (see Standing, 1979). It assumes inviscid (potential) flow and linear (small-amplitude) waves. Earlier investigations indicated that viscous effects were likely to have relatively little influence on wave-frequency motions, except possibly close to natural frequencies.

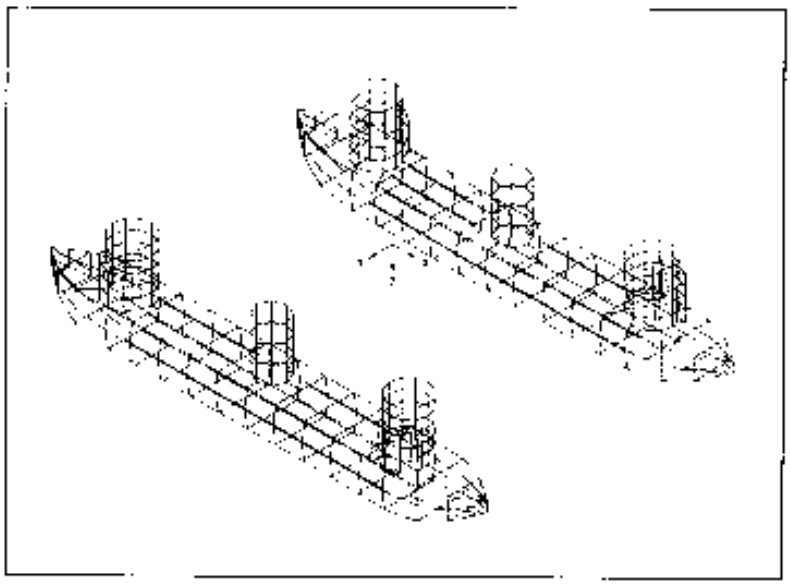

Figure 6
Numerical diffraction model of the 'Uncle John'

The outer surface of the two pontoons and six main columns was first divided into 668 facets or plane area elements, as shown in Figure 6. The program places a fluid source at the centre of each facet, pulsating at the same frequency as the incident regular waves. It then calculates source strengths required to satisfy the condition that the fluid velocity normal to the structure's surface should be zero. From these source strengths the program calculates the pressure distribution over the structure's surface, hence the hydrodynamic forces and moments, added masses and wave radiation damping coefficients. These terms are incorporated into linearised equations describing the vessel's response, which are then solved using a standard matrix inversion procedure.

All the calculations described in this paper were performed at the vessel's operating draught.

Bracing members made a relatively minor contribution to wave loads and motions, but were represented using a linearised version of Morison's equation to model both drag and inertial loads, as described by Wilson, Trim and Jackson (1987).

Wave forces, added masses, damping coefficients and response amplitude operators were then calculated for a range of regular wave periods and wave heading angles.

3.2 NUMERICAL INVESTIGATIONS

Variation of GM

Table 2 shows that the metacentric height GM varied between 2.15 and 2.53 m during the measurement programme. Some preliminary calculations were therefore performed, using, NMIWAVE, to investigate the sensitivity of the vessel's response motions to variations in GM. Calculations of the vessel's roll and pitch response amplitude operators (RAOs) were repeated using the two extreme values of GM. The results were often almost indistinguishable, and always quite close, and all further calculations were therefore performed using the larger GM value 2.53 m.

Short-crested seas

Wave conditions at sea were monitored using a conventional Waverider buoy, and so no wave directional information was available. A second numerical investigation was therefore performed using NMIWAVE, in order to find out whether the vessel's motions were likely to be sensitive to changes in the amount of wave directional spreading, and to investigate uncertainties in comparing the full-scale measurements with numerical predictions and laboratory data.

Comparisons were therefore made between numerical predictions from NMIWAVE in unidirectional and multidirectional waves, the latter defined by spreading functions of the form:

$$g(\theta - \bar{\theta}) = A\cos^n(\theta - \theta) \qquad \textbf{(1)}$$

where θ is the direction of the component wave, A is a normalisation constant, n is the spreading parameter, and θ is the mean wave direction. The calculations were repeated with n = 2, 6 and ω (unidirectional waves).

In order to allow meaningful comparisons to be made between these three cases, and also with measured transfer functions, the theoretical RAO $R(f, \theta)$ for individual unidirectional wave components was integrated over all wave directions θ defined by the wave spreading function g (θ - $\bar{\theta}$). The theoretical 'pseudo-transfer function' $\tilde{R}(f, \theta)$:

$$\tilde{R}(f, \tilde{\theta})^2 = \int_{\pi}^{\pi} R(f, \theta)^2 g(\theta - \bar{\theta}) d\theta \qquad \textbf{(2)}$$

was then compared directly with the transfer function between the measured response spectral density $S_R(f,\theta)$ and the point wave spectral density $S_\zeta(f)$:

$$\tilde{R}(f, \bar{\theta})^2 = \frac{S_R(f,\bar{\theta})}{S_\zeta(f)} \qquad \textbf{(3)}$$

For each mean direction $\bar{\theta}$ the results for n = 6 always lay between those for unidirectional waves and those with the widest spread, n = 2. Not surprisingly, the heave response showed least effect of wave spreading: the pseudo-transfer functions obtained for n = 0, 2 and 6 were generally almost indistinguishable. In this and other cases, however, the difference became larger at high wave frequencies in the quartering seas condition, $\theta = 45^o$. The multidirectional wave results were sometimes larger and sometimes smaller than those in unidirectional waves, but the differences between them were not large.

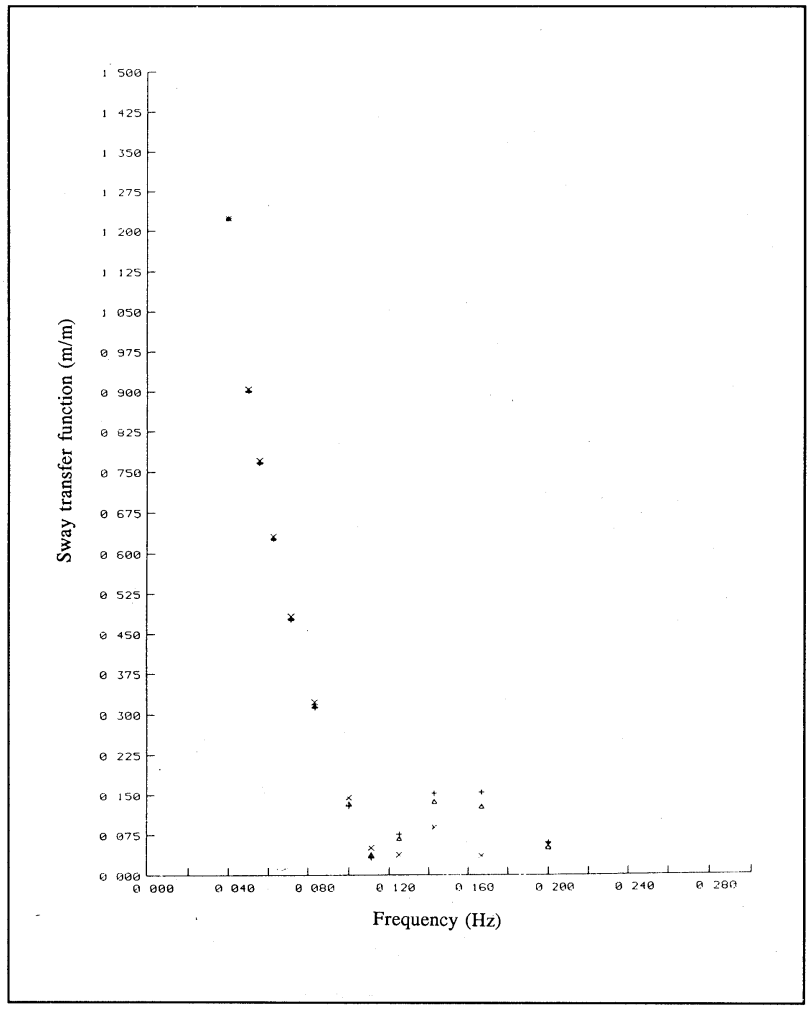

Figure 7
Theoretical 'pseudo-transfer functions' for sway response:
x *unidirectional;*
multidirectional: + n = 2,* Δ *n = 6

Figure 7 shows a sample comparison for sway response when $\bar{\theta} = 45^o$.

For the purpose of correlating the theoretical results with full-scale data the theoretical pseudo-transfer functions for n = 2 were chosen, these showing the largest effects of wave spreading. It was not realistic to represent wave spreading in the second-order, low-frequency study, to be described later, and this was based on a unidirectional analysis.

3.3 COMPARISON WITH MEASURED WAVE-FREQUENCY MOTIONS

Measured response amplitude operators were found to vary from one run to another, even where the wave conditions were nominally the same. Some of this variability comes from taking a finite sample from a stationary process, but other factors include uncertainties in the mean wave direction, which was only judged approximately by eye. There may also have been instances of crossing seas, or changes in the mean direction with frequency.

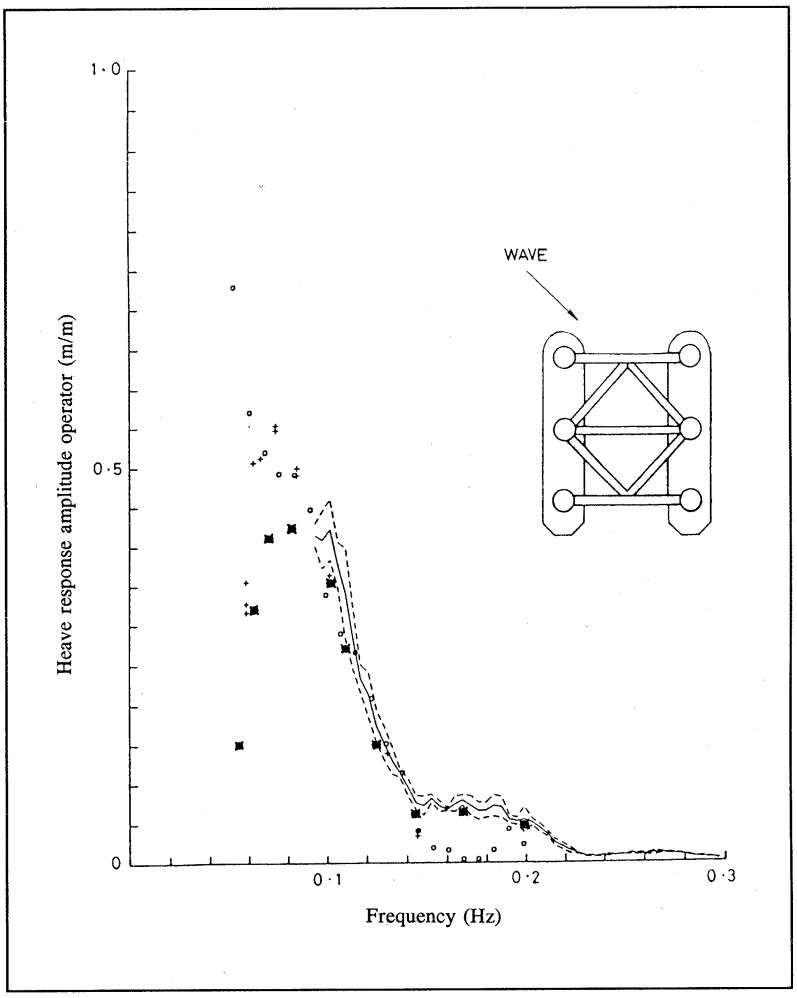

Figure 8
First-order heave RAOs:
_____ *mean full-scale, - - ± 1σ*
o + ***model tests; • NMIWAVE***

In order to improve the reliability of the RAO estimates, and reduce the variability from all such causes, the results from all measurement runs at nominally the same mean heading were combined together. The solid lines in Figures 8 and 9 thus represent the mean full-scale RAO, and the dashed lines represent one standard deviation $\pm\,\sigma$ either side of the mean. These Figures show typical heave and sway transfer functions in the quartering seas condition. The full-scale measured RAOs were found to correlate well with numerical results from NMIWAVE. The numerical RAOs shown in these two Figures represent the 'pseudo-transfer functions' $\tilde{R}(f,\bar{\theta})$, assuming a $\cos^2(\theta-\bar{\theta})$ distribution.

The laboratory model tests were performed in unidirectional waves. The differences observed between these results and the other two sets of data, for frequencies between 0.15 and 0.2 Hz, are largely consistent with differences seen earlier in the numerical calculations between unidirectional and multidirectional waves in this region (eg see Figure 7). The numerical values follow the full-scale mean measured RAO very well.

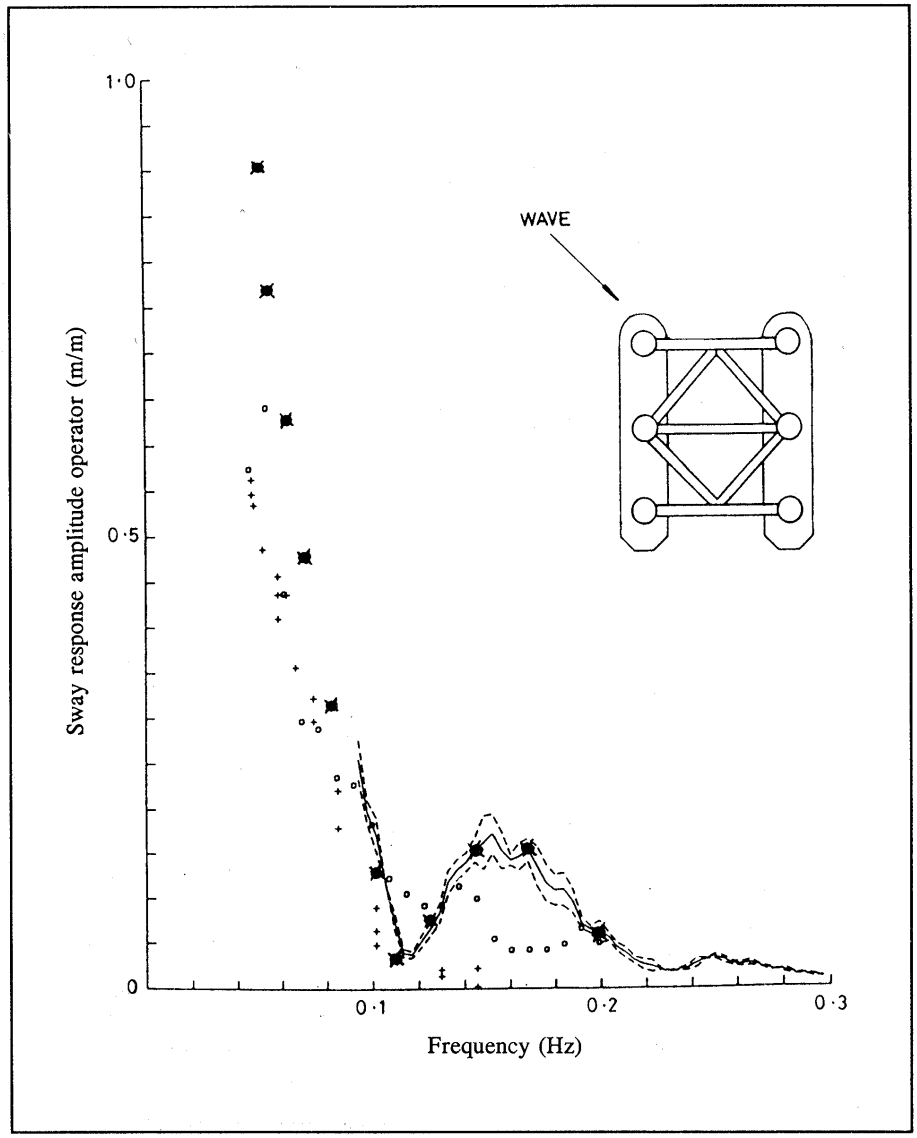

Figure 9
First-order sway RAOs for the 'Uncle John'
For key, see Figure 8

Somewhat larger discrepancies were noted in pitch and roll, as shown in Figure 10 for example. In these cases the laboratory model data tend to match up well with the numerical results, and the full-scale measured transfer functions in roll and pitch show larger variability at low frequencies than the results for the other motions, and also tend to approach a constant value at high frequencies. These may be indicative of greater levels of noise, measurement inaccuracy or sensitivity to variations in wave conditions.

Significant responses R_{sig} in the wave-frequency range were also calculated from the measured and theoretical response spectra. Table 3 compares a typical set of measured and calculated significant responses in a sea state with significant wave height 3.17 m and zero crossing period 5.86 sec. These values were calculated using the formulae:

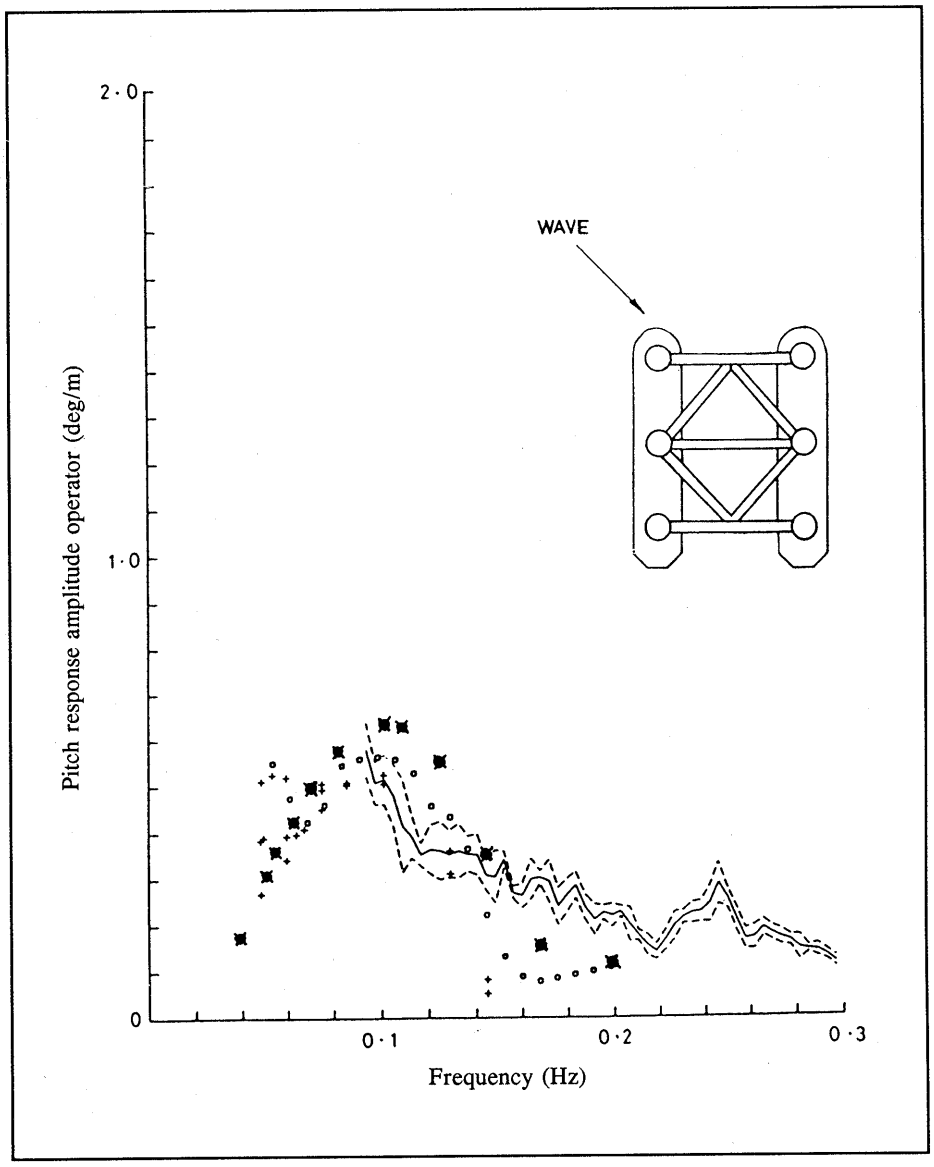

Figure 10
First-order pitch RAOs for the 'Uncle John'
For key, see Figure 8

$$R_{sig} = 4\sqrt{m_o}$$

$$m_o = \int_{f_a}^{f_b} S_R(f)df$$

where m_o represents the variance of the response, and the integration was over the frequency range 0.06 Hz to 0.2 Hz. The numerical results were obtained using a mean JONSWAP wave spectrum ($\gamma = 3.3$), with $\cos^2(\theta - \theta)$ spreading, together within RAOs for unidirectional waves from NMIWAVE.

Table 3
Wave-frequency significant responses for H_s = 3.17 m:
comparison between full-scale measurements and numerical predictions

	Full Scale	Predictions
surge (m)	0.18	0.22
sway (m)	0.34	0.35
heave (m)	0.48	0.42
roll (deg)	1.7	1.4
pitch (deg)	1.0	1.3

Figure 11 summarises significant responses in the wave-frequency range, from the full-scale measurement, shown as a function of significant wave height. These values are compared with model test data and with numerical predictions obtained using unidirectional and $cos^2(\theta - \bar{\theta})$ spread sea models. These results are for bow quartering wave condition. The numerical predictions generally agree well with the full-scale measured data, confirming results from the spectral analysis.

3.4 SHORT-TERM AND LONG-TERM EXTREME VALUE ESTIMATION

Designers and operators need to be able to estimate the extreme responses of the vessel, and these tend to be sensitive to any non-linearities presents. The analysis therefore included an assessment of methods for estimating both short-term and long-term extreme values. The techniques used and results obtained are described in detail by Wilson, Trim and Jackson (1987).

Short-term estimates were first made of extreme responses from three successive runs in a sea-state of 3½-hours duration, with approximately stationary conditions and H_8 = 3.20m. These time-histories were first filtered to remove the low-frequency response; maxima and minima from all three runs were then calculated, and the maximum out-to-out response was assumed to be the maximum minus the minimum value. This assumption is consistent with narrow-band spectral assumptions, though in practice the maximum and minimum values will not usually be consecutive.

These values were found to agree very closely, in all five modes of motion (surge, sway, heave, roll and pitch), with theoretical estimates of expected maximum responses in the same sea-state, based on the well-known Longuet-Higgins asymptotic formula. The level of agreement is probably at least partly fortuitous, bearing in mind likely statistical uncertainties.

Long-term estimates were also made for 10 and 25-year return periods, based on the maximum likelihood method and on a Gaussian model. The maximum likelihood estimates almost always fitted the measured up-crossing rate functions better than the Gaussian model. The results clearly demonstrated the sensitivity of estimated return values to the shape of the tail of the up-crossing rate function, with the suggestion that the Gaussian model might lead to a significant underestimation of extreme values. It is important to remember, however, that these results were obtained from very short measurement periods of just a few days, and so cannot provide quantitatively reliable estimates of 10 and 25-year return values.

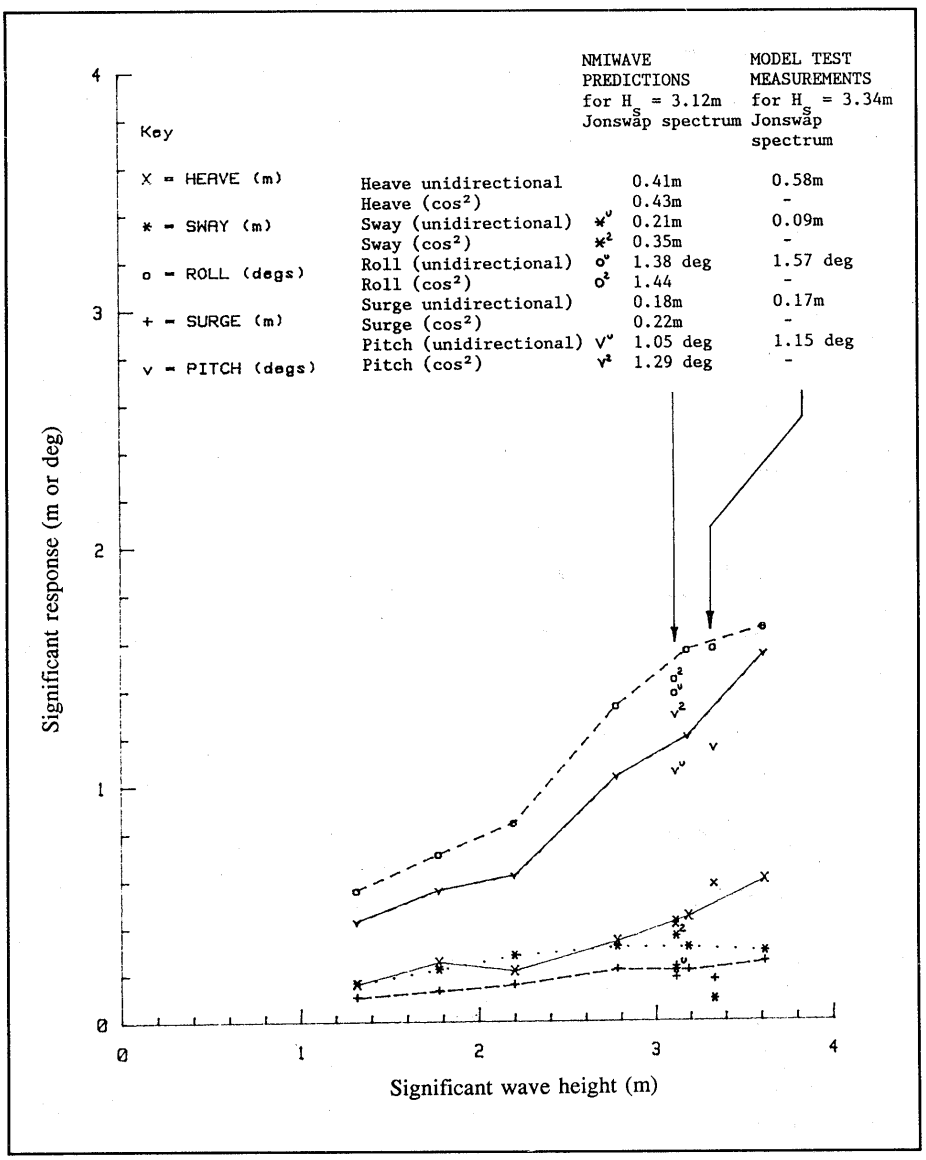

Figure 11
Wave-frequency significant responses
full-scale measurements compared with model test data and NMIWAVE predictions

4. LOW-FREQUENCY MOTIONS

The original purpose of the full-scale measurement programme, and the one for which the measuring equipment was designed, was to assess first-order wave-frequency motions. Early on, however, it became apparent that a large part of the vessel's response was at frequencies below the range of major wave activity. Figure 12, for example, shows the total measured significant response of the 'Uncle John', as a function of significant wave height. These values are larger, in some cases very much larger, than those shown in Figure 11, which were calculated from the wave-frequency component of the response only.

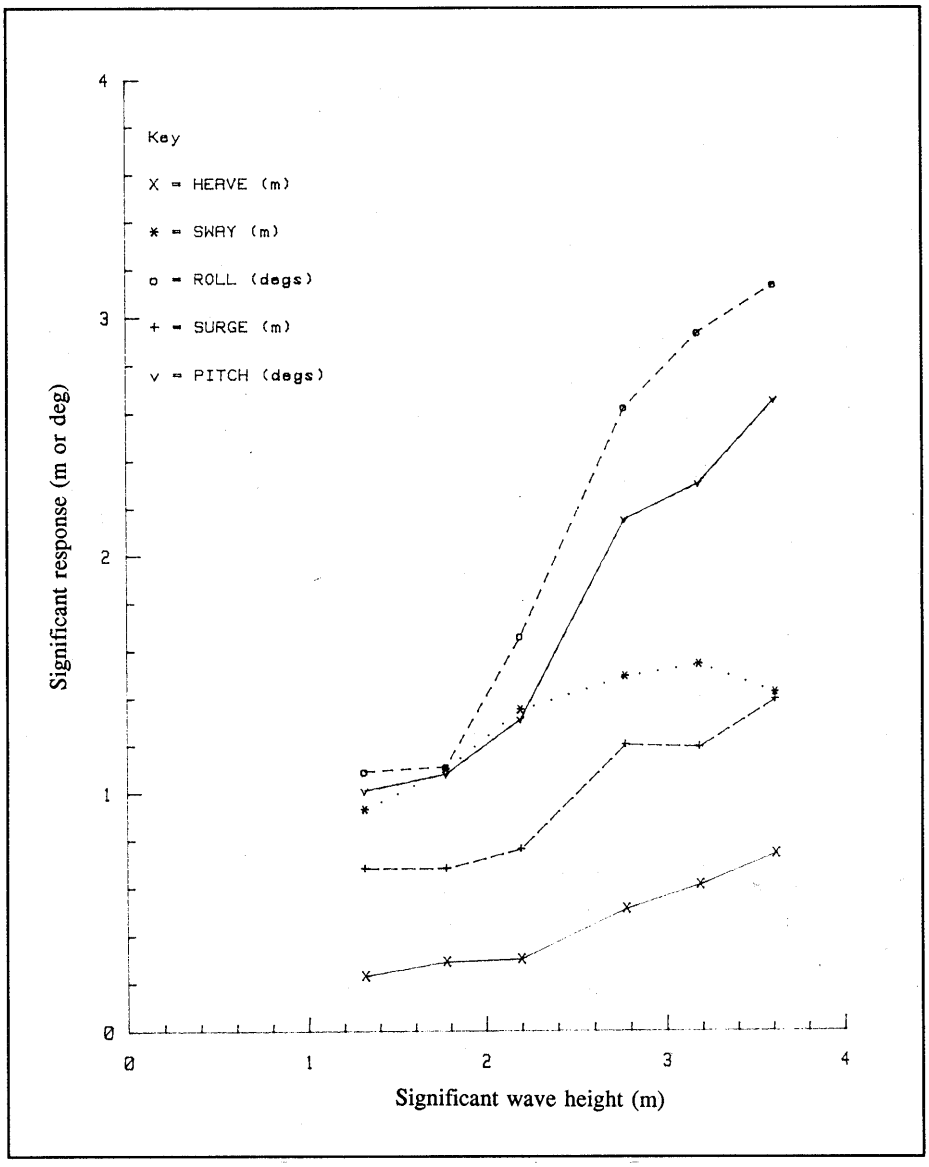

Figure 12
Total significant full-scale measured responses

Table 4
Full-scale measured significant responses:
comparison between low-frequency and wave-frequency components

	Low-frequency	Wave-frequency
surge (m)	1.47	0.23
sway (m)	1.39	0.29
heave (m)	0.47	0.54
roll (deg)	2.49	1.65
pitch (deg)	2.09	1.44

Table 4 shows a typical set of significant responses, obtained using equations (4) and integrating over the low-frequency (0.0 to 0.08 Hz) and wave-frequency (0.08 to 0.24 Hz) ranges separately. These results correspond to a sea state with significant wave height H_8 = 3.65 m. The low-frequency responses are generally larger than the wave-frequency contributions, and this is especially true in surge and sway.

Encouraged by the level of agreement found in the wave-frequency range, BMT attempted a similar analysis of low-frequency motions. Low-frequency motions were considered likely to be due to a combination of second-order or other non-linear wave loads, swell waves and low-frequency wind gust loading. The mechanisms proved, however, to be much more complex and difficult to understand than those associated with first-order motions. A summary of the results of the low-frequency motion analysis has been published by Standing, Brendling and Jackson (1991), and full details may be found in the main report on the project by Brendling and Standing (1990).

Twenty-four measurement runs were selected for analysis, in all of which the vessel was at its operational draught of 15.5 m. These runs were selected either around the height of the second storm, or to give fairly long periods of steady sea conditions. Wind and wave conditions during these four sequences are shown in Table 5.

Sequences B and C represent runs from around the peak of the second storm, in which the vessel was able to remain on station, at its operational draught and under DP control. Sequence A and D represent more moderate wave or wind conditions respectively, in which the measured motions were relatively small and the results correspondingly less reliable than during the storm. Most of the sample results and conclusions in this report correspond to sequence B conditions, though results for sequences A, C and D are contained in two of the summary tables.

Table 5
Run numbers, wind and wave conditions selected for analysis

Sequence	Run nos	Wind direction (deg)	Mean Wind speed (m/s)	Significant wave height (m)
A	85 - 94	80	11	1.2
B	131 - 134	135	17	3.2
C	136 - 140	165	19	3.1
D	158 - 162	105	8	1.8

The instrumentation package included accelerometers to measure surge, sway and heave accelerations. The signals from the accelerometers were double-integrated to provide surge, sway and heave displacements. Independent estimates of the surge and sway motions were available from a taut wire system which was part of the vessel's normal station-keeping equipment. It was found that wave-frequency surge and sway motions could be obtained reliably from the accelerometer package. This system was not sufficiently sensitive to provide low-frequency surge and sway motions, however, and these motions had to be obtained from the vessel's taut wire system.

It is not easy to estimate the accuracy of surge and sway measurements obtained in this way. Recordings were obtained after the taut wire signals had been filtered by the dynamic positioning control system to remove the wave-frequency component. This means that there are two potential sources of error: in the measurement itself, and from the filtering process. The accuracy of the taut wire (angular) measurement was quoted to be about ±0.05 degrees, and in the relevant water depth this implies a surge or sway accuracy of ±0.04 m. There are further possible inaccuracies due to current and wave forces on the wire, catenary effects, stiction in still water, and due to roll and pitch motions of the vessel. Overall, the absolute accuracy of the low-frequency and sway motion measurements was considered to be about ±0.1 to 0.2 m. Although measured motions were generally not much larger than this, the accuracy of the standard deviation of response was probably rather better than ±0.1: firstly because consistent errors, such as those due to current loads on the taut wire, were likely to affect mean offsets rather than time-varying motions, and secondly, because random error were 'averaged out' by the process of calculating the standard deviation.

Wind speed was obtained from an anemometer device fitted to the vessel to provide a 'wind feed forward' input to the dynamic positioning system. Time-histories of wind forces and moments were calculated using instantaneous values of wind speed $V_w(t)$ at time t, combined with the appropriate force or moment coefficient $C_x(\psi_w)$ obtained from the earlier wind-tunnel tests, as follows:

$$F_x(t) = \tfrac{1}{2} \rho_a A_x C_x (\psi_w) V_w^2(t) \qquad -5$$

where ρ_a is the air density, A_x is the presented area in the appropriate direction and ψ_w is the wind direction relative to the vessel.

The Waverider buoy was moored about 500 m away from the vessel. Wave records at the vessel's location were, therefore, not available. The numerical model therefore

simulated wave time-histories with the same statistics and spectra as the full-scale records, but not the same time-histories. This meant that the calculated and measured response time-histories could not be compared directly, but only in a spectral or statistical manner.

The theoretical model used in this investigation represents one fairly typical approach to design, and describes low-frequency responses due to second-order wave loading and wind gusting. The aim during this investigation was to make the model sufficiently realistic to allow meaningful and detailed comparisons to be made with the full-scale measured motions. The model therefore incorporated measured properties of the actual vessel and environment. These properties included actual measured wind and wave time-histories (or frequency spectra derived from them), together with information about the full-scale vessel's heave, roll and pitch damping, and characteristics of its dynamic positioning control system.

4.1 HEAVE, ROLL AND PITCH MOTIONS

Like most semi-submersibles the 'Uncle John' has a fairly small waterplane area, and the natural periods in heave, roll and pitch (see Table 2) are quite long. The wave buoy system was not able to measure very long-period waves, but it seemed unlikely that the amount of long-period swell present would be sufficient to excite a large resonant response. The contributions from wind and from second-order wave loading were therefore investigated.

Low-frequency motions in these three modes are primarily associated with resonant responses. An essential step in developing the theoretical model was therefore to estimate the vessel's damping characteristics. Damping coefficients were identified from the measured response histories by means of the synthetic decrement technique (see Brendling and Wilson, 1987). The theoretical model then reproduced the average rate of decay of the measured correlation function. This procedure made no assumption about the magnitude of the forcing. Comparisons between measured and calculated responses could therefore be used to assess the validity of the theoretical force calculation procedure.

The resulting estimates of damping varied considerably from run to run, and it was not possible to assign a precise value for each mode of motion. Five percent of critical was judged, somewhat subjectively, to be a reasonable estimate of the average damping in all three modes, although estimates varied typically between half and double this value. Theoretical predictions were based throughout on five percent of critical damping in heave, roll and pitch.

The vessel's low-frequency heave, roll and pitch motions, caused by unsteady wind gusting, were then estimated using a simple linear, single-degree-of-freedom, frequency-domain spectral model, together with force coefficients derived from earlier wind-tunnel experiments.

Response due to second-order low-frequency wave forces and moments were also calculated, using mean wave drift force coefficients from the NMIWAVE model used in the first-order investigation, and using the Newman (1974) approximate formula as derived by Pinkster (1974):

$$S_F(w) = 8 \int_o^\infty F_D^2(\overline{w}, \overline{w}) S(w^1) S(w + w^{1)} dw^1 \qquad -6$$

Where $F_D(\overline{w}, \overline{w})$ represents the mean force in regular waves of unit amplitude at the mean frequency $\overline{w} = w^1 + \frac{1}{2}w$, and S($w1$) is the wave spectral density at angular frequency w_1. The force coefficients were calculated using the so-called 'near-field' method (Standing and Dacunha, 1982).

Table 6 summarises the standard deviations of the wind and wave drift contributions to the calculated heave, roll and pitch responses, together with a combined estimate obtained using a 'square root of sum of squares' formula. These estimates are compared with the total measured responses. Each of the measured items in this Table represents the root mean square of values obtained from individual runs within each sequence. The standard deviation for each individual run was evaluated using equation (4), integrating between 0.01 and 0.075 Hz.

Table 6

Mean values of the standard deviations of low-frequency heave, roll and pitch responses: comparison between measurements and theoretical calculations based on wind and second-order wave forces

Motion component	Data source	Run sequence			
		A	B	C	D
Heave (m)	Measured	0.050	0.092	0.107	0.036
	Calculated				
	- Wind	0.005	0.015	0.016	0.003
	- Waves	0.005	0.109	0.101	0.023
	- Combined	0.007	0.110	0.102	0.024
Roll (deg)	Measured	0.110	0.493	0.575	0.211
	Calculated:				
	- Wind	0.057	0.092	0.078	0.031
	- Waves	0.017	0.043	0.038	0.020
	- Combined	0.060	0.101	0.087	0.037
Pitch (deg)	Measured	0.077	0.427	0.444	0.176
	Calculated:				
	- Wind	0.026	0.078	0.125	0.012
	- Waves	0.008	0.067	0.066	0.018
	- Combined	0.027	0.102	0.141	0.022

The wind-induced heave response was found to be very small, and heave motions in the three higher sea states (sequences B, C and D) were due mainly to second-order wave forces, and were predicted remarkably well by the numerical model. This level of agreement may be partly fortuitous, bearing in mind the fairly large uncertainties in values of damping and other parameters, and also comment (v) below.

Figure 13 compares a typical measured heave response spectrum, obtained in a sequence B sea state, with the theoretical spectrum due to second-order wave forces only. This Figure shows a clear misalignment of the measured and predicted peaks. In earlier investigations on semi-submersible and similar vessels (see comments by

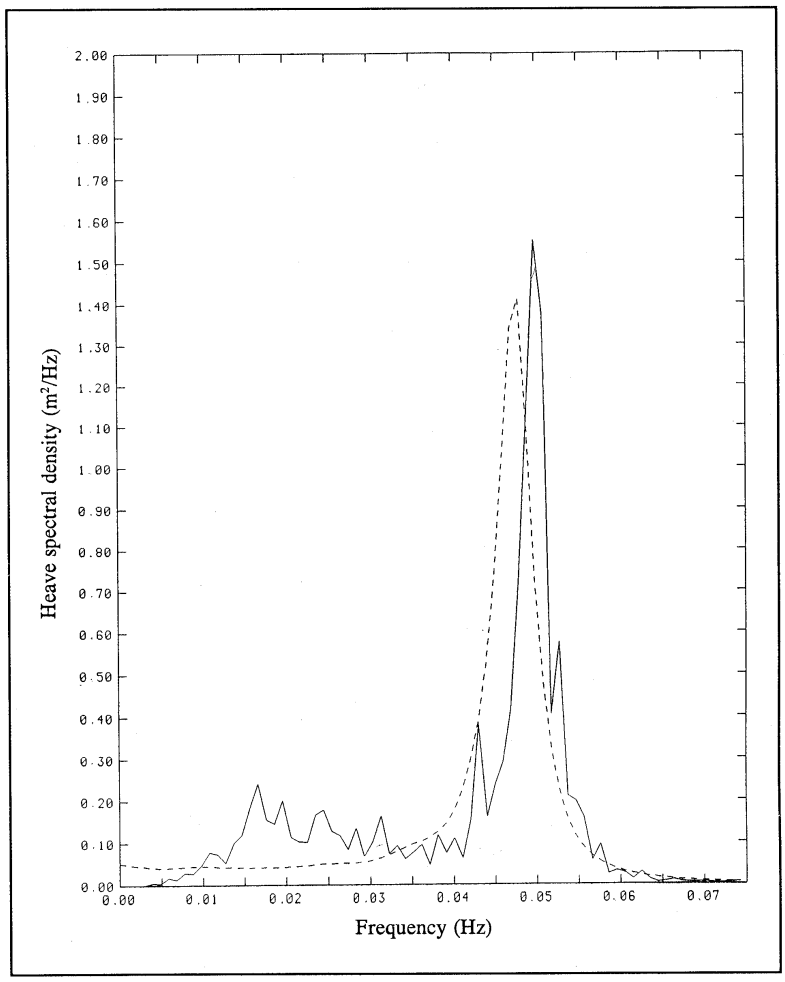

Figure 13
Low-frequency heave response spectra:
_____ *full-scale measurements,*
- - second-order wave force theory

Standing, 1990) three-dimensional wave diffraction programs were found to overestimate the heave added mass and heave natural period. The same tendency is apparent here.

The measured spectrum also shows a secondary broad peak below the natural heave frequency. This secondary peak was probably caused by measurement noise, associated with the double integration and subsequent filtering of accelerometer signals. The level of noise is nonetheless quite low, despite the small magnitude of the measured motions.

Figures 14 and 15 show typical roll and pitch response spectra corresponding to the same sequence B state. Once again these Figures compare full-scale measured spectra with theoretical estimates based on second-order wave forces only. The theoretical spectra lie well below the measured spectra, although the measured and predicted natural roll and pitch periods agree quite well. Table 6 shows that wind

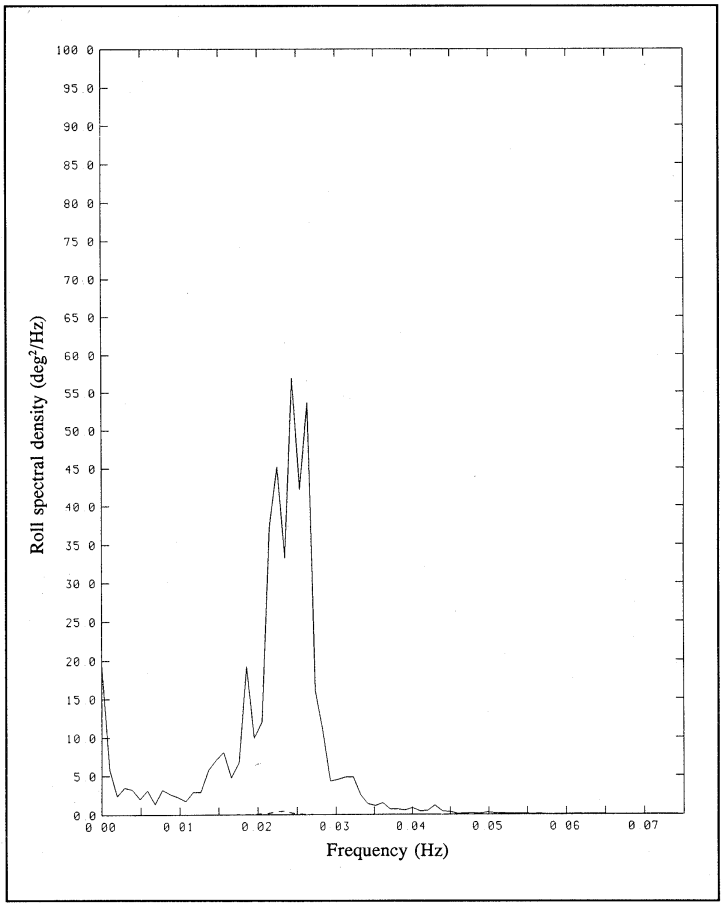

Figure 14
Low-frequency roll response spectra:
--- *full-scale measurements,*
-- second-order wave force theory

loads generally made a larger contribution than second-order wave forces, but account for at most 30 to 50 percent of the standard deviation of measured low-frequency pitch and roll responses.

The combined predicted responses to wind and second-order wave loads were often found to be less than the measured motions. There are several possible contributory factors:

(i) The calculated second-order wave forces were based on inviscid flow assumptions, and made no allowance for drag. Drag is likely to affect low-frequency responses more than first-order, wave-frequency motions (See Section 5 below), and is likely to affect the roll and pitch components more than heave.

(ii) The damping estimated by the synthetic decrement approach showed considerable scatter, and may have been overestimated. A purely qualitative comparison of the shapes of the spectral peaks, however, suggested that errors in the damping were insufficient to explain the discrepancies.

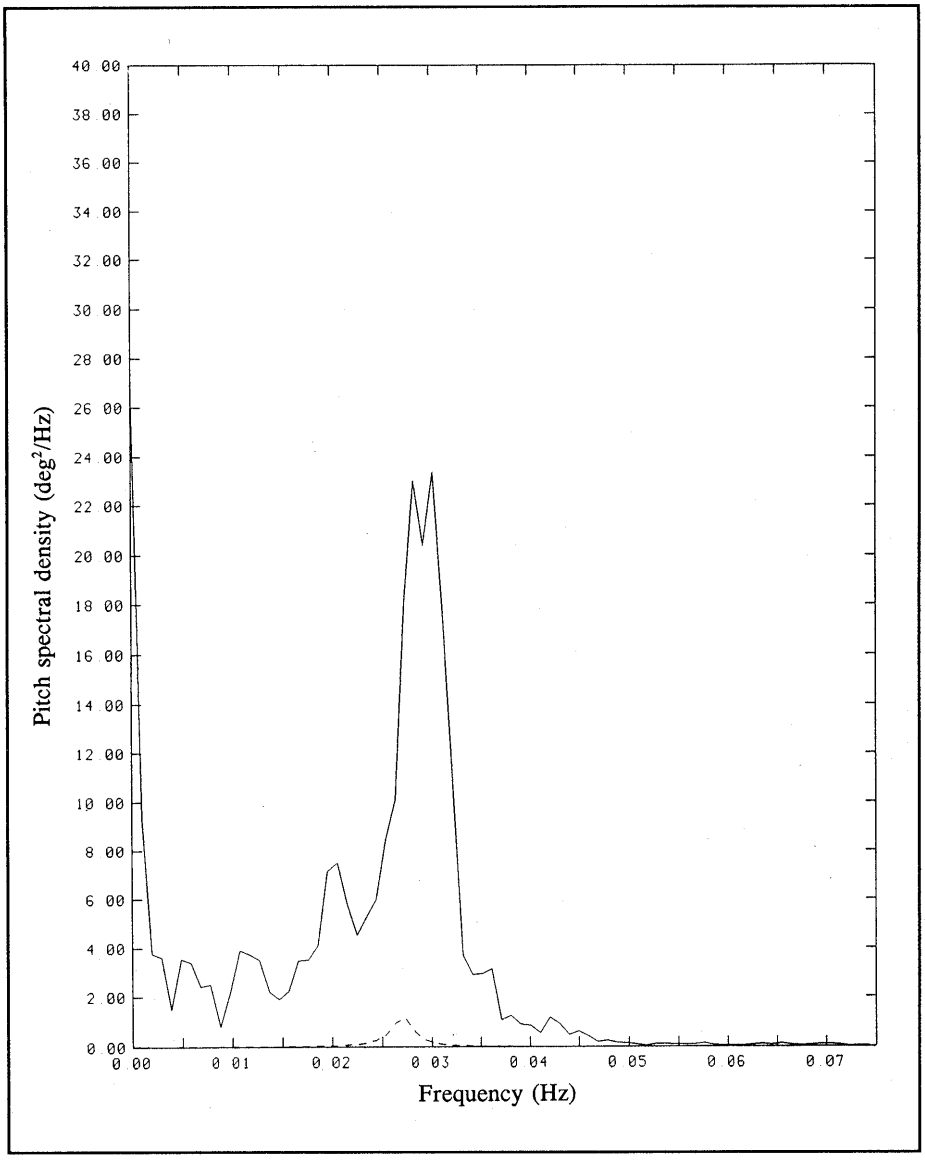

Figure 15
Low-frequency pitch response spectra:
--- full-scale measurement,
-- second-order wave force theory

(iii) Motions of the actual vessel may have been excited directly by long-period swell waves, which the Waverider buoy was unable to measure reliably. Swell would probably have affected heave motions more than pitch and roll, however, and heave was quite well predicted using a second-order wave force model. ignoring swell.

(iv) Roll and pitch motions may have been excited directly by the thrusters.

(v) Numerical accuracy of the second-order forces and of the the Newman approximation (equation 6) were not investigated, but are a possible source of error. Kim and Yue (1991), for example, showed that the Newman approximation can seriously underestimate second-order, low-frequency forces and moment on deep-draughted vertical cylinders in long waves.

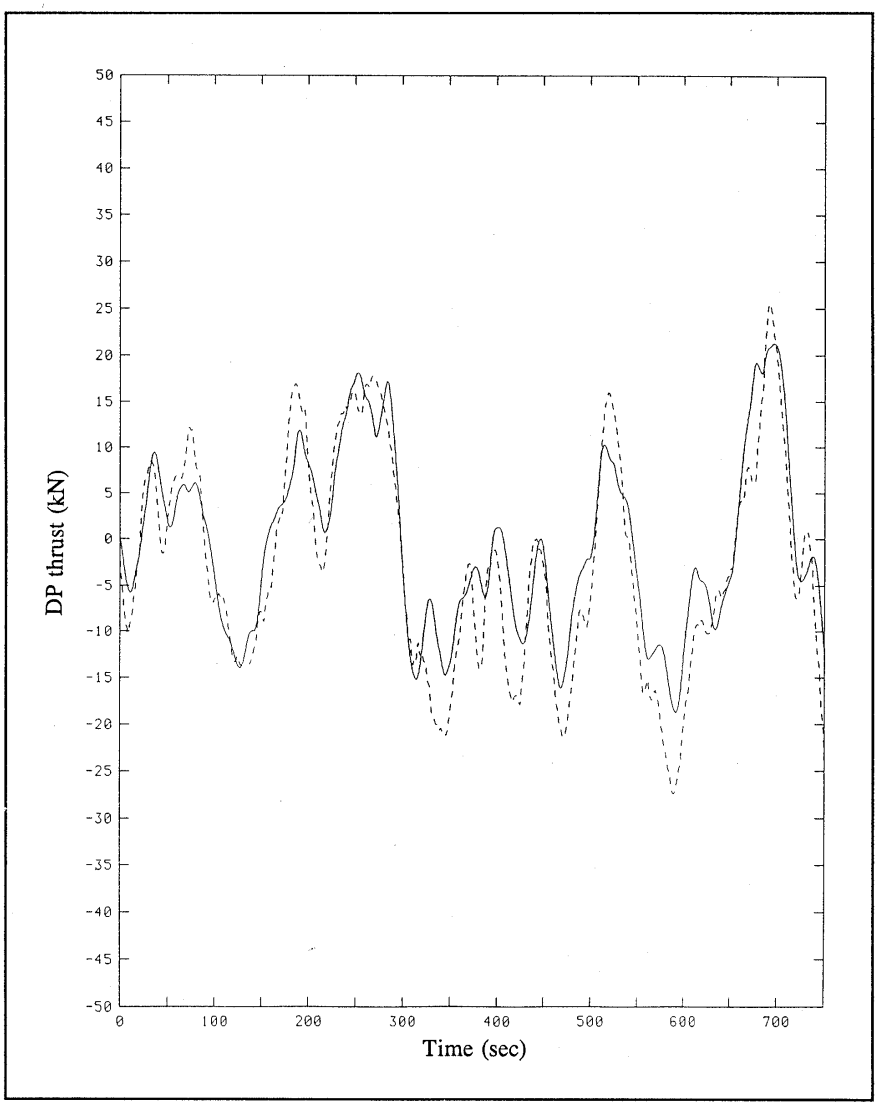

Figure 16
Thrust demand in the sway direction:
_____ full-scale measurement,
- - numerical simulation from measured sway

4.2 SURGE AND SWAY MOTIONS

The measured surge and sway motion spectra showed significant amounts of energy at frequencies below 0.01 Hz. The magnitudes of these low-frequency surge and sway motions depend on the performance of the vessel's dynamic positioning system. After early unsuccessful attempts to develop a simplified simulation model of this system, characteristics of the PID controller used on board the actual vessel were represented, including maximum limits applied to the differential and integral terms, and to the total thrust available.

Figure 16 compares typical measured and predicted time-histories of the thrust demand signal in the sway direction. It compares the thrust demanded by the actual and simulated control systems, both in response to the *measured* sway motion. The

two time-histories agree well, confirming that the numerical model correctly reproduces the performance of the full-scale control system.

The measured signal in Figure 16 represents the thrust demanded by the controller, and does not necessarily represent the force actually applied to the vessel by the thrusters. There are many possible reasons for differences between the demanded and actual thrust, including the response time of the thrusters, and hydrodynamic interactions between thrusters, and between the thrusters and hull. These effects were ignored in the present investigation, though may have a bearing on the final conclusions.

There were several other differences between the simulated and actual systems. The full-scale control system includes filters to remove wave-frequency components from the offset error signal before calculating the thrust demand. These filters may have introduced further delays into the control process. A filter was not used in the simulations model, because the program calculates low-frequency motions only.

The vessel's low-frequency surge and sway motions were simulated using the BMTSPM program, which modelled wind gust loads, second-order low-frequency wave drift forces together with the control and thruster system. The BMTSPM program is a general-purpose time-domain simulation package, the fundamentals of which have been described by Brendling and Wilson (1987).

Very little information was available about the current speed (other than evidence that it was small), and it was ignored in this investigation. Hydrodynamic damping from the vessel's hull was also ignored, partly because it was unknown, and partly because the thrusters were considered likely to be the main source of damping.

Wind forces were calculated using the actual measured wind speed history, together with force coefficients obtained from earlier wind tunnel tests. Some initial numerical simulations, modelling wind loads only, demonstrated the major advantages of having a 'wind feed forward' system installed on board the vessel. When the 'wind feed forward' system was switched on, the resulting thruster forces almost exactly balanced the external wind forces, and the vessel hardly moved. The two sets of forces almost exactly balance in the simulation model, because the same wind force coefficients are used to drive the 'wind feed forward' controller and to calculate the wind force history. In reality, of course, the 'wind feed forward' system does not exactly balance the external wind force:

a) because the actual wind force differs from that predicted using the simple quasistatic formula (equation 5); and

b) because the dynamic positioning controller and thrusters cannot respond instantaneously to changes in wind speed and direction, causing a time lag between the wind force and the 'wind feed forward' thrust.

These effects were ignored in the present investigation, but may have a bearing on the final conclusions.

Second-order, low-frequency wave drift forces were added to the simulation model. Mean force coefficients were first calculated using the NMIWAVE program and the 'near-field' approach. The force time-histories were simulated using the 'geo-mean' approximation, rather than the related and more conventional Newman approximation (equation 6). The 'geo-mean' approximation, described by Brendling

and Wilson (1987), involves replacing the quadratic transfer function FD(w_1, w_2) by the expression:

$$F_D(w_1, w_2) = \tfrac{1}{2}\{sgn[F_{Do}(w_1)] + sgn[F_{Do}(w_2)]\} \times \sqrt{|F_{Do}(w_1)F_Do(w_2)|}$$

where F_{Do} (w) is the mean force in regular waves of unit amplitude and angular frequency w, and sgn[F_{Do}] = ± 1 depending on the sign of F_{Do}.

Table 7 summarises the standard deviations of measured surge and sway responses, compared with values obtained from the numerical simulations. Each item in this Table represents the mean of values obtained from individual runs within each sequence. These values were obtained using equation (4), integrating over the low-frequency range between 0.0 and 0.03 Hz.

This Table shows that numerical model underpredicted the surge and sway responses in every case, though sometimes achieved 50 percent of measured values.

Table 7
Mean values of the standard deviations of low-frequency surge and sway responses: comparison between measurements and numerical simulations

Motion component	Data source	Run sequence			
		A	B	C	D
Surge (m)	Measured	0.382	0.874	1.138	0.480
	Calculated	0.048	0.427	0.569	0.066
Sway (m)	Measured	0.290	0.864	0.976	0.361
	Calculated	0.104	0.228	0.176	0.175

Figures 17 and 18 compare typical measured and predicted surge and sway response spectra, in a typical sequence B sea state, due to combined wind and second-order wave forces. The numerical model has underestimated the response, though the general shapes of the spectra are approximately correct, suggesting that the measurements are likely to be reliable, and that some features of the numerical model are likely to be valid.

In an earlier investigation, Standing et al (1990) compared simulated low-frequency response of a moored semi-submersible with small-scale model test data, *both in unsteady wind alone*. It was found that the numerical model overestimated surge response.

Possible factors contributing to discrepancies between measured and predicted surge and sway responses include the following:

(i) The calculated second-order wave forces were based on inviscid flow assumptions, and made no allowance for drag. Drag is likely to affect low-frequency responses more than first-order, wave-frequency motions (see Section 5 below), and is especially likely to affect the surge and sway responses.

(ii) Wind forces acting on the full-scale vessel may have differed from those calculated by the 'wind feed-forward' system.

(iii) The numerical model may have responded more rapidly to station-keeping errors than the full-scale vessel, where delays may have been introduced as a result of filtering the measured offsets or in initiating thruster action.

(iv) Numerical accuracy of the second-order forces and of the geo-mean approximation were not investigated, but are a possible source of error.

(v) The accuracy of the measured motions, obtained from the vessel's taut wire system, is probably only about ±0.1 to 0.2m.

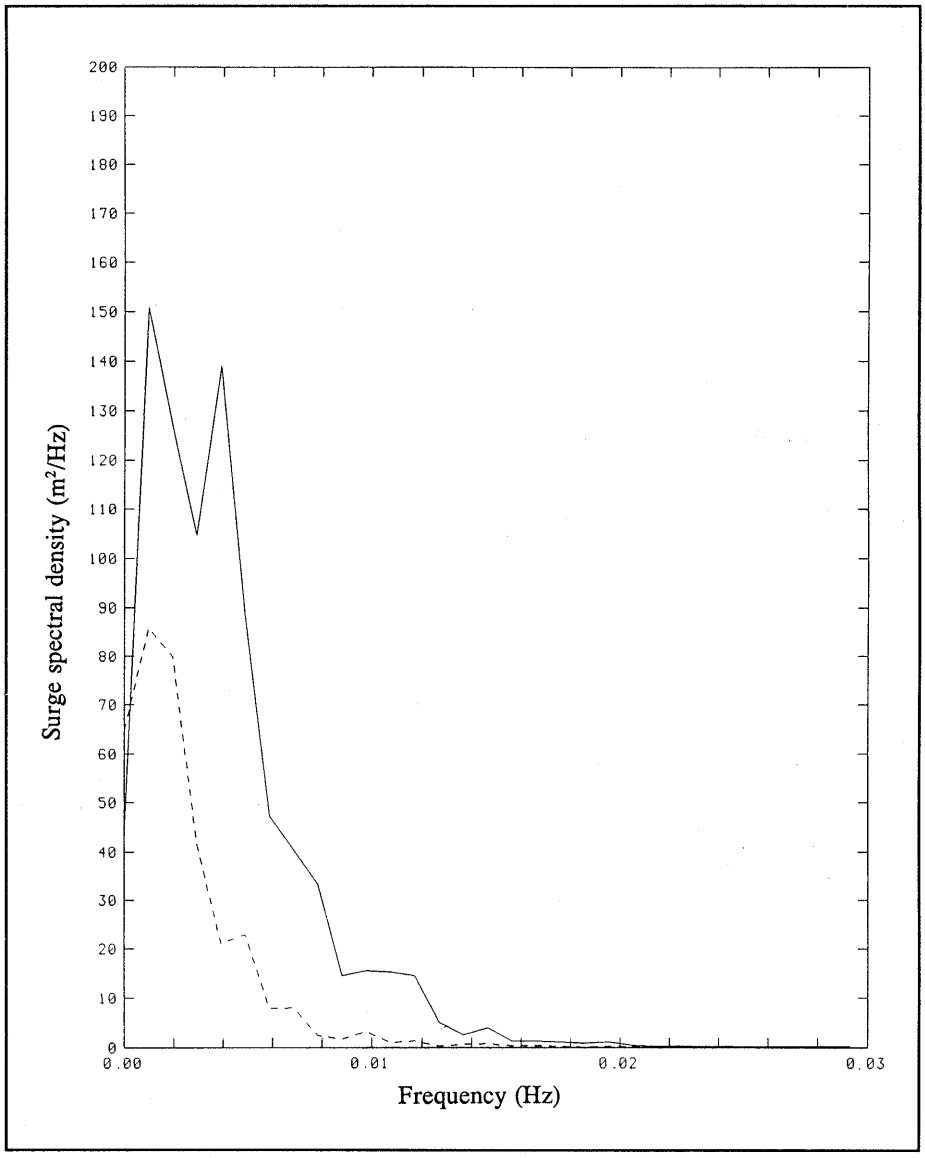

Figure 17
Low-frequency surge response spectra:
_____ full-scale measurement
-- numerical simulation

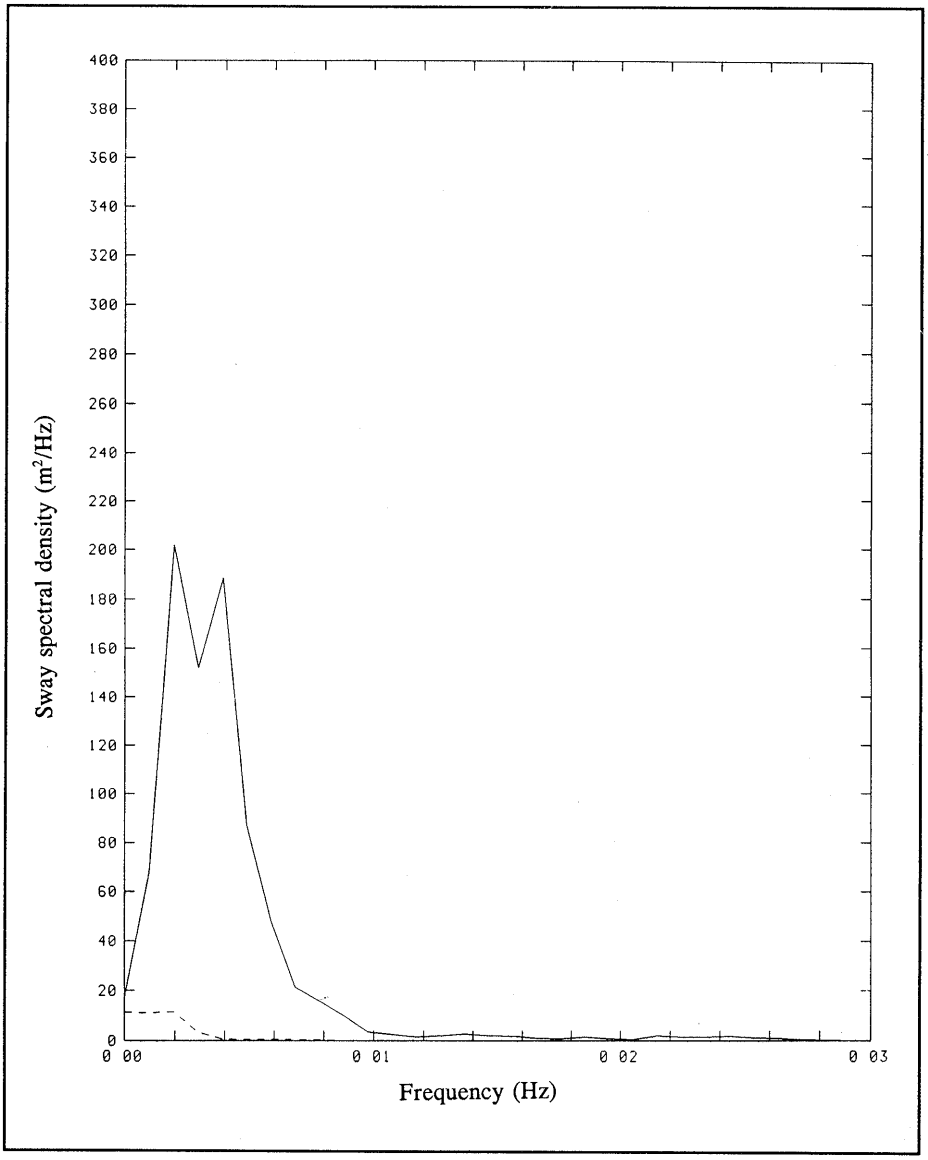

Figure 18
Low-frequency sway response spectra:
--- full-scale measurement,
-- numerical simulation

5. VISCOUS DRAG

The wave drift force coefficients used in the BMTSPM simulations, described in Section 4, were obtained using the NMIWAVE diffraction program, in which the mean and low-frequency forces represent second-order effects of wave diffraction and radiation. The mean horizontal force, for example, is associated with changes in the momentum of the diffracted and radiated wave field.

The NMIWAVE model is based on potential flow assumptions, and does not represent viscous effects such as skin friction, flow separation, vortex-shedding and drag. Huse (1977) demonstrated that viscous drag can sometimes affect the mean and low-frequency drift behaviour of a semi-submersible, the importance of drag increasing with wave height. Viscous drag was therefore investigated as possible source of discrepancies between the predicted low-frequency motions, measured motions of the full-scale vessel and laboratory model data.

It proved impractical, within the constraints of the project, to calculate drag forces on the complete structure during a full motion simulation. Some simplified additional calculations were performed in order to investigate the relative magnitudes of the drag and potential flow contributions to the wave drift force, and the likely validity of the simulation procedure that had been adopted.

The mean drag force on the vessel was estimated from forces acting on the six individual legs, ignoring loads on the pontoons. The procedure took account of first-order relative velocities and changes in relative surface elevation. Both of these relative motion effects proved to be significant.

The mean drag force on a single leg of diameter D in regular waves of angular frequency *w* was estimated using the approximate formula:

$$\tfrac{1}{2}C_d\rho D u_o^2 \zeta_o \tfrac{1}{T}\int_o^T \cos(wt)|\cos(wt)|\cos(wt-\in)dt \qquad (8)$$

$$= \tfrac{2}{3\pi}C_d\rho D R_u^2 R_\zeta \zeta_a^3 \cos(\in)$$

where C_d is the drag coefficient, u_o is the relative horizontal velocity amplitude, ζ_o is the amplitude of the relative surface elevation, $\in$ is the phase lag between the relative surface elevation and velocity, ζ_a is the amplitude of the undisturbed incident wave, and $R_u(w)$ and $R_\zeta(w)$ are the response amplitude operators for relative velocity and surface elevation. Contributions to the drag force from all six legs were then added together.

Figure 19 shows three alternative numerical estimates of the mean wave force in the surge direction, compared with data measured on a laboratory model of the 'Uncle John' in regular waves. The mean surge force $\overline{F_x}$ is expressed as a non-dimensional coefficient:

$$\overline{F}_x \backslash \rho g \zeta_a^2 L \qquad (9)$$

where ρ is the water density, g is the acceleration due to gravity, ζ_a is the wave amplitude and L is the vessel's length. The solid line represents wave drift forces calculated by the NMIWAVE program, based on potential flow assumptions alone

(C_d = 0.0). The two dashed lines show alternative increases in the mean force associated with viscous drag, calculated using equation (8) with C_d = 0.7 and 2.0. The latter value might be appropriate to model-scale conditions, where the members are rough, or of square or rectangular section. The smaller value, 0.7, would be more appropriate to smooth circular cylinders at full scale. The two curves may therefore be regarded as bounding the likely range of forces at model and full scales.

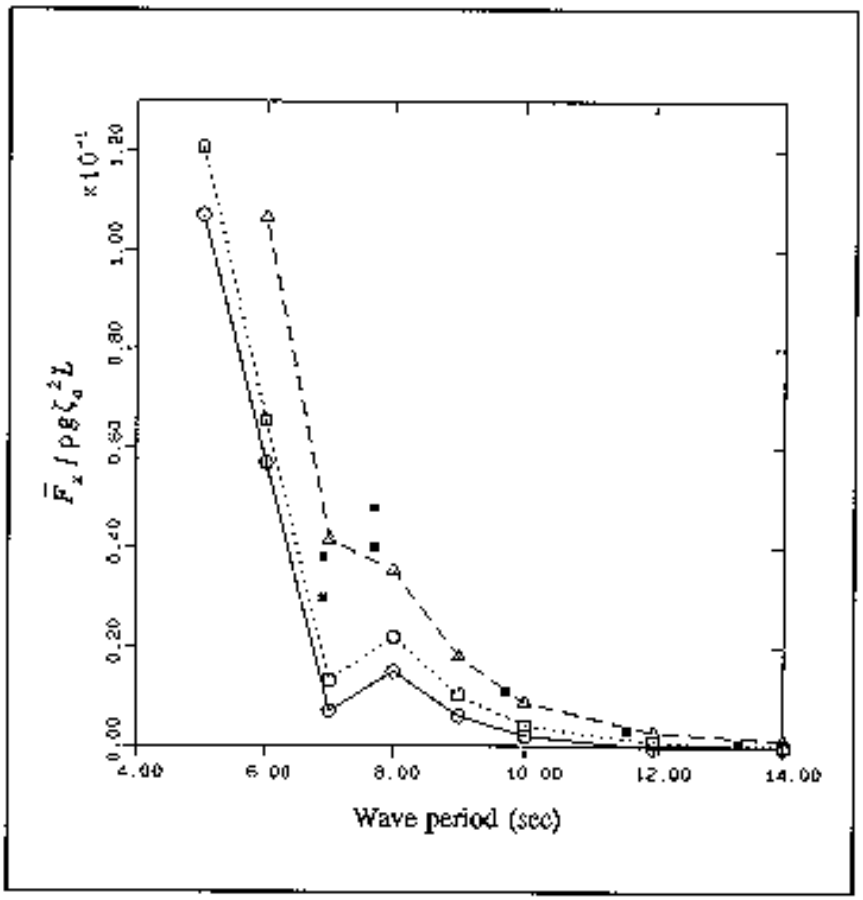

Figure 19
Mean surge force:
___o___ *C_d = 0.0 (NMIWAVE)* -□- *0.7*, -Δ- *2.0*
■ *model tests*

The theoretical curve, obtained using C_d = 2.0, does in fact agree quite well with the model test data. These results suggest that viscous drag can indeed make a significant contribution to the mean wave force, at least at model scale, and probably also at full scale.

Low-frequency surge force time-histories (but not vessel responses) were then simulated in irregular waves, taking account of drag forces acting between the mean and instantaneous water surfaces. Figure 20 compares theoretical exceedance distributions of forces, based on a typical measured wave history. The dashed line is based on first-order diffraction calculations and potential flow assumptions, with no viscous drag component; the dotted line represents the drag force contribution alone, with $C_d = 0.7$. The solid line represents the sum of the two terms. The effect of drag would, of course, be even larger if a drag coefficient closer to that indicated by the model test data in Figure 8 had been used, but a value of 0.7 was considered closer to industry practice for estimating drag forces on the main legs, which are of approximately circular section. The forces were calculated using equation (8), together with the Hsu and Blenkarn (1970) approximate simulation procedure, in which the second-order force during each half wave cycle was assumed to be the same as the mean force in a regular wave of the same amplitude and half-period.

The result suggest that viscous drag is likely to be one of perhaps several significant factors causing differences between the predicted and measured motions.

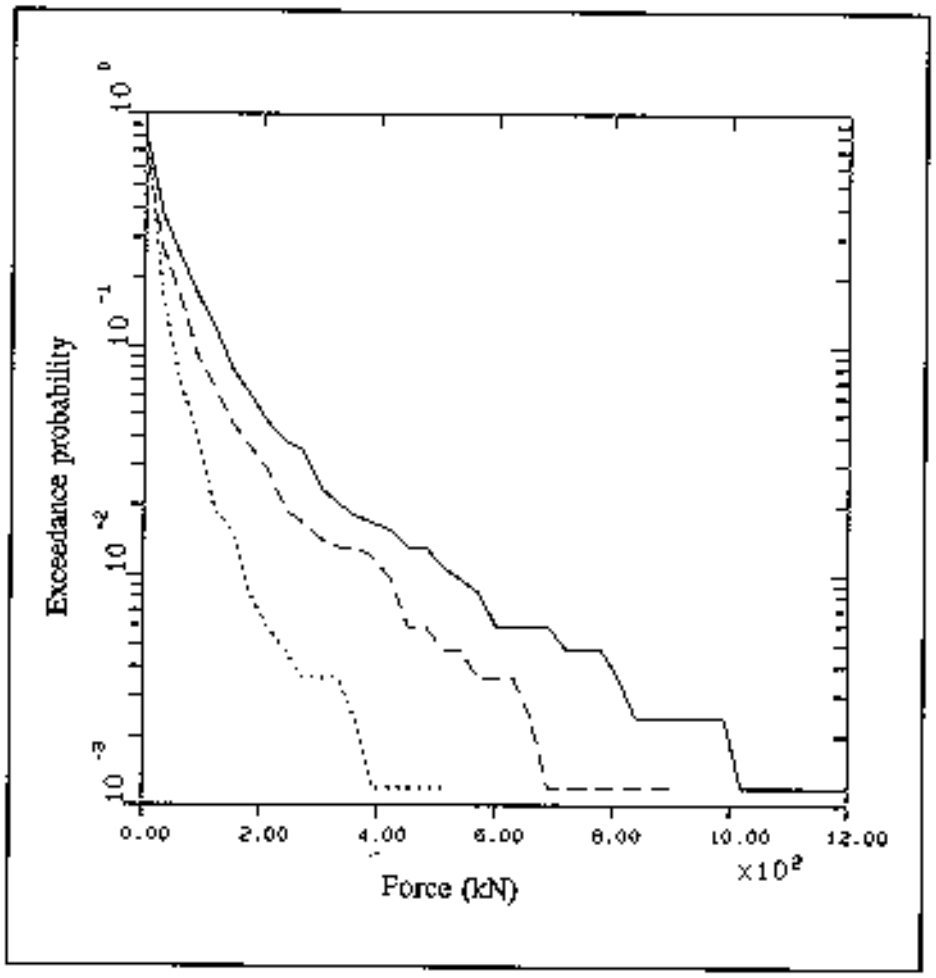

Figure 20
Exceedance distributions of low-frequency surge force:
-- potential flow alone, ... drag force, ____ total force

6. CONCLUDING COMMENTS AND RECOMMENDATIONS

Motions of the dynamically positioned Semi-Submersible Support Vessel 'Uncle John' were measured while it was operating in the North Sea. Wave-frequency and low-frequency components of these motions were then correlated with theoretical predictions. The purpose of the present investigation was to improve understanding of these processes and of the limitations of the theoretical model. Models of this type are increasingly being used in the design of mooring and dynamic positioning systems. Where the safety of a design is based upon such a model, its reliability needs to be established. These investigations showed that theoretical estimates of low-frequency motions should be used with great caution.

Full-scale measured wave-frequency motions generally correlated well with numerical predictions obtained using the NMIWAVE diffraction program, both in terms of the significant responses and in terms of the spectra. Discrepancies were noted in some of the spectra at high frequencies, which may be associated with wave directional spreading. Both the full-scale data and numerical model included wave directional spread, whereas laboratory model tests had been performed in unidirectional waves. Slightly larger differences to the pitch and roll spectra may indicate measurement noise or sensitivity to vessel or sea conditions.

Low-frequency motions were assessed separately, using a theoretical model combining low-frequency wind gust loads and second-order wave forces, calculated under inviscid potential-flow assumptions. This model also represented response charactericstics of the actual full-scale vessel, including its heave, roll and pitch damping, and its dynamic positioning control system with maximum thrust limits in surge and sway.

This model predicted very well the vessel's low-frequency heave motions in higher sea states, and up to 50 percent of the measured surge and sway responses. These motions were found to be due mainly to second-order wave forces. Wind gust loading was found to account for at most 30 to 50 percent of the vessel's roll and pitch responses. Wind forces in the horizontal direction were significant, but were largely balanced, at least in the numerical model, by thruster forces from the 'wind feed forward' system.

The theoretical model often underestimated low-frequency motions, especially in the roll, pitch, surge and sway directions. Possible contributory factors, requiring further detailed investigation, include:

- viscous drag forces, which were not represented in the theoretical model,
- inaccuracy of modelling certain features of the thruster and control systems, in particular delays caused by thruster action and filtering,
- differences between actual wind forces acting on the vessel and those calculated by its 'wind feed forward' system,
- low-frequency swell, which could not be measured reliably,
- thruster-induced roll and pitch,

- uncertainties in the amount of damping, and numerical modelling uncertainties,

- uncertainties in the measured surge and sway motions.

The magnitudes of these differences, and the general uncertainty surrounding them, is not surprising in view of difficulties widely reported elsewhere in estimating low-frequency and second-order motions. This is still an area of active research, with large uncertainties surrounding the mechanisms of forcing, damping and response, and how they should be calculated. Comparisons between results from different commercially-available computer programs have shown large differences between numerical estimates of responses (see, for example, Nielsen et al, 1990).

It is important to obtain maximum benefit from this fairly unique set of high-quality data. It is recommended, therefore, that the measured data should be analysed further in an attempt to decide the most likely causes of the observed differences, and, if possible, to make recommendations on numerical modelling procedures. This further analysis should include sensitivity studies where the measurements are insufficient to provide clear diagnostic information.

As a later state it may be appropriate to repeat some of the measurements, with equipment specially designed to investigate specific aspects of the problem, but at this stage a further measurement programme would seem premature.

The results of the present investigation point to certain deficiencies in the theoretical model and measurements, but say very little about the design and performance of the 'Uncle John' itself. This vessel was designed on a different basis from that described here, and has performed consistently well over many years. Furthermore the operations of the 'Uncle John', as a diving support vessel, are limited mainly by its heave response. This turned out to be more predictable than the other motions, with a greater proportion of wave-frequency response.

The results of this investigation do, however, suggest caution in the use of theoretical procedures of the type described here when designing future semi-submersibles, particularly in situations where the limiting motions are likely to be surge and sway, and where careful design of the dynamic positioning system is critical to safe and economic operation.

ACKNOWLEDGEMENTS

The authors gratefully acknowledge the assistance of Houlder Offshore Ltd, who made the 'Uncle John' itself available for the measurement programme, together with data from previous investigations, and their permission to publish these results. Particular thanks are due to Mr R.L.F. Smith and the vessel's crew. The authors would also like to thank the Petroleum Engineering Division of the Department of the Energy and the Offshore Safety Division of the Health and Safety Executive who provided financial support.

REFERENCES

Brendling W J and Wilson D, 1987, 'Theoretical and experimental investigation of the low frequency motions of a single anchor leg moored buoy and tanker', Workshop on Floating Structures and Offshore Operations, MARIN, Wageningen.

Brendling W J and Standing R G, 1990, "Uncle John' low frequency motion analysis. Final report', BMT report to the Department of Energy, project no 35204, OT-N-90125.

Every M J, 1988, "Uncle John' motion measurement at full scale - executive summary', BMT report to the Department of Energy, project no 30013, OT-O-88002.

Haavie T O and English J W, 1978, 'Design of a special purpose North Sea support vessel', Trans North East Coast Institu Engrs and Shipbldrs, vol 94.

Houlder J M, 1981, "Uncle John': a semi-submersible multi-purpose support vessel for oil exploration and production', Trans Instit Marine Engrs (TM), vol 94, paper no 18.

Hsu F H and Blenkarn K A, 1970, 'Analysis of peak mooring force caused by slow vessel drift oscillation in random seas', Offshore Technology Conf paper no OTC 1159, Houston.

Huse E, 1977, 'Wave induced mean force on platforms in direction opposite to wave propagation', Norwegian Maritime Research, vol 5, no 1, pp 2-5.

Jackson G E, 1987, "Uncle John' motion measurement. Report no 1: instrumentation and preliminary full-scale results', BMT Report to the Department of Energy, project no 30013, OT-N-88109.

Jackson G E and Wilson D, 1988, 'Full-scale measurements on the semi-submersible 'Uncle John'', Offshore Technology Conf paper no OTC 5824, Houston.

Kim H M and Yue D P, 1991, 'Sum-and-difference-frequency wave loads on a body in unidirectional Gaussian seas', J Ship Res, vol 35, no 2, pp 127-140.

Morch M, Kaasen K E and Rudi H, 1983, 'Full-scale measurements of free-oscillation motions of two semisubmersibles', Offshore Technology Conf paper no OTC 4532, Houston.

Newman J N, 1974, 'Second-order slowly-varying forces on vessels in irregular waves', Proc Symp. Dynamics of Marine Vehicles and Structures in waves, Inst Mech Engrs, London.

Nielsen F G, Herfjord K and Loken A, 1990, 'Floating production systems in waves. Results from a comparative study on hydrodynamic coefficients, wave forces and motion responses', Norsk Hydro Report no R-043812, Bergen.

Olsen O A and Verlo P O 1976, 'A comparison of full-scale performance measurements of Aker H-3 with theoretical predictions', Offshore Technology Conf paper no OTC 2508, Houston.

Pinkster J A, 1974, 'Low-frequency phenomena associated with vessels moored at sea', Soc Petr Engrs, AIME, paper no SPE 4837.

Standing R G, 1979, 'Use of wave diffraction theory with Morison's equation to compute wave loads and motions of offshore structures', National Maritime Instit, report no R74, Dept of Energy report no OT-R-7607.

Standing R G and Dacunha N M C, 1982, 'Slowly-varying and mean second-order wave forces on ships and offshore structures', Proc 14th ONR Symp Naval Hydrodynamics, Ann Arbor.

Standing R G, 1990, 'The verification and validation of numerical models, with examples taken from wave diffraction theory, wave loading and response', Proc IUTAM Symp on Dynamics of Marine Vehicles and Structures in Waves, Brunel University, Uxbridge.

Standing R G, Wills J A B and Singh S, 1990, 'Wind loading and dynamic response of a floating production platform in waves', Conf on Environmental Forces on Offshore Structures and their Prediction, Soc for Underwater Technology, London, Kluwer Academic Publishers, pp 351-382.

Standing R G, Brendling W J and Jackson G E, 1991, 'Full-scale measured and predicted low-frequency motions of the Semi-Submersible Support vessel 'Uncle John'', Proc 1st ISOPE Intl Conf Offshore and Polar Engrg, Edinburgh Vol III, pp 434-441.

Wilson D, Trim A and Jackson G E, 1987, ''Uncle John' motion measurements. Report 2: comparison of full scale, model test and theoretical data', BMT Report to the Department of Energy, project no 30013, OT-O-88001.